

計畫編號：NHRI-EX97-9735EI

國家衛生研究院整合性醫藥衛生科技研究計畫

根據虛擬電極之人工電子耳刺激策略的神經生理研究

計畫名稱

97年度成果報告

執行機構：國立交通大學

計畫主持人：蔡德明 教授

本年度執行期間： 97 年 1 月 1 日 至 97 年 12 月 31 日

全文處理方式：二年後對外提供參考

本研究報告僅供參考用，不代表本院意見

計畫編號：NHRI-EX97-9735EI

國家衛生研究院整合性醫藥衛生科技研究計畫

根據虛擬電極之人工電子耳刺激策略的神經生理研究

計畫名稱

97年度成果報告

執行機構：國立交通大學

計畫主持人：蔡德明 教授

本年度執行期間： 97 年 1 月 1 日 至 97 年 12 月 31 日

全文處理方式：二年後對外提供參考

本研究報告僅供參考用，不代表本院意見

目錄

項目	頁碼
壹、97 年度計畫研究成果摘要	1
貳、97 年度計畫著作一覽表	2
參、97 年度計畫重要研究成果產出統計表	3
肆、97 年度計畫重要研究成果	4
伍、97 年度計畫所培訓之研究人員	5
陸、參與 97 年度計畫所有人力之職級分析	6
柒、參與 97 年度計畫所有人力之學歷分析	7
捌、參與 97 年度計畫之所有協同合作之研究室	8
玖、97 年度計畫執行情形	9
拾、附錄	10
拾壹、97 年度之著作抽印本或手稿	11

壹、97年度計畫研究成果摘要

計畫名稱：根據虛擬電極之人工電子耳刺激策略的神經生理研究

計畫編號：NHRI-EX97-9735EI

執行機構：國立交通大學

計畫主持人：蔡德明

研究人員：曲在雯，孫樹海，詹竣傑，陳正誼，蘇育廷，徐建華，李彥廷，蔡雯雅，蔡宗儒，王怡翔，鄒宜霖

關鍵字：人工電子耳，虛擬電極，神經生理學，動物實驗

成果分類： 癌症基礎與臨床研究(可複選，最多三項)

分子與基因醫學研究

臨床研究

生物技術與藥物研究

生物統計與生物資訊研究

醫療保健政策研究

環境衛生與職業醫學研究

醫學工程研究

老年醫學研究

精神醫學與藥物濫用研究

疫苗研究

幹細胞研究

奈米醫學研究

其他重要疾病或醫藥衛生問題研究

(1) 中文摘要

國外研究指出在安靜環境中，人工電子耳使用者只需要 6 至 9 個有效的頻道就有足夠聽力聽到大多數英語談話。但是目前人工電子耳系統只有 16 或 22 電極是不足夠給人工電子耳使用者聽(或欣賞)音樂、聽國語或在吵雜環境中使用。最新的研究指出增加頻譜信息與時域信息能增進人工電子耳使用者在吵雜環境中、聽音樂、聽國語等聽力的效能。本計畫提出以虛擬電極提高有效的頻道數量及頻譜信息。

本計畫第一年重點是架設人工電子耳硬體與軟體的研究平台、驗證兩個電極與四個電極的虛擬電極電流操控演算法，並開發在動物研究上所使用的測試電極與架設量測聽學誘發電位平台。

(2) 英文摘要

Though cochlear implants have been commercial available products, there are still a lot of questions regarding how to improve the hearing capability of cochlear implant (CI) patients. The two major factors that affect the hearing performance of CI patients are temporal cues and spectral cues they receive. While it is possible to increase the temporal cues by raising the electrical stimulating rate, the spectral cues the CI patients receive is limited by the number of electrode contacts. The current available number of electrode contacts in a cochlear prosthesis system is 16 or 22, it is proposed to raise the number of functional electrode by means of virtual channels (or current steering).

Research shows that while 6 to 9 effective channels are sufficient for hearing and understanding English speech in quiet environment, however, it is not enough for listening to speech in noise, music and tonal language, particularly Mandarin Chinese.

The first year of this project is focused on setting up a hardware and software cochlear implant research platforms, validating the 2 electrode and 4 electrode current steering algorithm, developing a test electrode for animal studies, and set up an auditory evoked potential (AEP) measurement platform.

貳、97年度計畫著作一覽表

Journal

序號	計畫產出名稱	產出型式	Impact factor	致謝對象
1	C. T. M. Choi and C. H. Hsu Conditions for Generating Virtual Channels in Cochlear Prosthesis Systems. Annals of Biomedical Engineering 2008; Supported by NHRI-EX97-9735EI (SCI) Revised	Foreign	2.3	NHRI

Patent

序號	計畫產出名稱
	無

Book

序號	計畫產出名稱
	無

Conference Paper

序號	計畫產出名稱
1	C.T. M. Choi, Y. T. Lee, Modeling Deep Brain Stimulation, The 13th International Conference on Biomedical Engineering/NHRI-EX97-9735EI 2008
2	C.T. M. Choi, C.H. Hsu, W.Y. Tsai and Yi Hsuan Lee, A Vocoder for a Novel Cochlear Implant Stimulating Strategy Based on Virtual Channel Technology, The 13th International Conference on Biomedical Engineering/NHRI-EX97-9735EI 2008
3	C.T. M. Choi, Y. T. Lee, Deep Brain Stimulation, Annual Conference of the Biomedical Engineering Society of ROC/NHRI-EX97-9735EI 2008
4	Modeling and Measurement of Various C.T. M. Choi, Y.C. Huang, T.S. Lian, C.W. Chen, Electrodes for Electrical Stimulation, Annual Conference of the Biomedical Engineering Society of ROC/NHRI-EX97-9735EI 2008
5	W.Y. Tsai, C.H. Hsu, Y.H. Lee, C.T.M. Choi, Vocoder Implementation of a Novel Cochlear Implant Stimulating Strategy, Annual Conference of the Biomedical Engineering

	Society of ROC/NHRI-EX97-9735EI 2008
--	--------------------------------------

Technical Report

序號	計畫產出名稱
	無

參、97年度計畫重要研究成果產出統計表

註：群體/中心計畫者，不論是否提出各子計畫資料，都必須提出總計畫整合之資料

(係指執行97年度計畫之所有研究產出結果)

科技論文篇數			技術移轉			技術報告 0 項		
發表地點 類 型	國 內	國 外	類 型	經 費	項 數	技術創新 0 項		
期 刊 論 文	0 篇	1 篇	技 術 輸 入	0 千元	0 項	技術服務 0 項		
研 討 會 論 文	3 篇	2 篇	技 術 輸 出	0 千元	0 項	專 利 權	國 內	0 項
							國 外	0 項
專 著	0 篇	0 篇	技 術 擴 散	0 千元	0 項	著 作 權	國 內	0 項
							國 外	0 項

〔註〕：

期刊論文：指在學術性期刊上刊登之文章，其本文部份一般包含引言、方法、結果、及討論，並且一定有參考文獻部份，未在學術性期刊上刊登之文章（研究報告等）與博士或碩士論文，則不包括在內。

研討會論文：指參加學術性會議所發表之論文，且尚未在學術性期刊上發表者。

專 著：為對某項學術進行專門性探討之純學術性作品。

技術報告：指從事某項技術之創新、設計及製程等研究發展活動所獲致的技術性報告且未公開發表者。

技術移轉：指技術由某個單位被另一個單位所擁有的過程。我國目前之技術轉移包括下列三項：一、技術輸入。二、技術輸出。三、技術擴散。

技術輸入：藉僑外投資、與外國技術合作、投資國外高科技事業等方式取得先進之技術引進國內者。

技術輸出：指直接供應國外買主具生產能力之應用技術、設計、顧問服務及專利等。我國技術輸出方包括整廠輸出、對外投資、對外技術合作及顧問服務等四種。

技術擴散：指政府引導式的技術移轉方式，即由財團法人、國營事業或政府研究機構將其開發之技術擴散至民間企業之一種單向移轉（政府移轉民間）。

技術創新：指研究執行中產生的技術，且有詳實技術資料文件者。

技術服務：凡有關各項研究計畫之規劃與評審、技術督察與指導及專業技術服務事項等。

肆、97年度計畫重要研究成果

註：群體/中心計畫者，不論是否提出各子計畫資料，都必須提出總計畫整合之資料

計畫之新發現、新發明或對學術界、產業界具衝擊性(impact)之研究成果，請依性質勾選下列項目。

- 1. 研發或改良國人重要疾病及癌症的早期診斷方式及治療技術
- 2. 發展新的臨床治療方式
- 3. 發展新生物製劑、篩檢試劑及新藥品
- 4. 瞭解常見疾病及癌症之分子遺傳機轉
- 5. 瞭解抗癌藥劑對癌細胞之作用機制
- 6. 提供有效的疾病預防策略
- 7. 利用生物統計與生物資訊研究，推動台灣生技醫藥研究，促進生物技術與基因體醫學之發展
- 8. 醫療保健政策相關研究
- 9. 瞭解環境毒理機制及重金屬對人體健康的影響
- 10. 研發適合臨床使用的人造器官及生醫材料
- 11. 縮短復健流程並增加復健效果的醫療輔助方式或器材之研究應用
- 12. 改進現有醫療器材的功能或增加檢驗影像的解析能力
- 13. 其他重要疾病或醫藥衛生問題研究

- 一、計畫之新發現、新發明或對學術界、產業界具衝擊性 (impact) 之研究成果，請敘述其執行情形。

We have found that it is necessary to move the electrode contact away from the modiolus to enhance the performance of the virtual channels. This is contradicting the current teaching that electrode needs to hug the modiolus to improve the performance of the cochlear implant system.

This result needs to be validated by electrophysiology animal experiments and by retro-study on published cochlear implant studies.

- 二、計畫對民眾具教育宣導之研究成果 (此部份將為規劃對一般民眾教育或宣導研究成果之依據，請以淺顯易懂之文字簡述研究成果，內容以不超過 300 字為原則)

市面上現有的人工電子耳使用 12 至 22 個電極刺激病患聽神經。但是研究指出目前人工電子耳系統只有 12 或 22 電極是不足夠給人工電子耳使用者聽(或欣賞)音樂、聽國語或在吵雜環境中使用。最新的研究指出增加頻譜信息與時域信息能增進人工電子耳使用者在吵雜環境中、聽音樂、聽國語等聽力的效能。

使用虛擬電極可以增加等效的電極數量及增加頻譜信息。一般人工電子耳電極陣列被設計緊靠在耳蝸軸上，也就是人類內耳的部份，因此可以使用最小的電流去刺激聽神經纖維。本研究計劃發現虛擬電極可以透過遠離耳蝸軸的電極而產生。這樣的治療方法是不同於世界其他的人工電子耳研究中心的方法。

本研究需要更多實驗結果去驗證。

- 三、簡述年度計畫成果之討論與結論，如有技術移轉、技術推廣或業界合作，請概述情形及成效

We have been discussing collaboration and technology transfer with the cochlear implant manufacturers, but it will require more validation before the manufacturers are interested. They require at least a small scale human clinical trial as a proof of concept which I have been working on. I have been collaborating with 振興醫院/新光醫院 on a small clinical trial (outside this NHRI project). The goal is to show that using a 500 channels stimulating strategy will improve pitch perception of cochlear implant patients.

- 四、成效評估（技術面、經濟面、社會面、整合綜效）

We have set up a CI research platform, finished preliminary work on electrophysiology experiment using animals, finished analyzing virtual channel schemes using two-electrode and four-electrode in the first year of the project. Since this is first year of the three year project, the impact of the accomplishment should be expected to be less than the last year of the project. We also have published based on the preliminary results. We have made good progress with respect to our targets and achieved good preliminary results.

- 五、下年度工作構想及重點之妥適性

The work on the cochlear implant (CI) research platform will continue. We will develop another CI research platform based on PDA and a new interface. This is needed since proprietary software and architecture used

by the cochlear implant manufacturers are hindering the progress of the CI research platform development. We feel the PDA, which has an open architecture, would allow us to develop better and more useful system for CI experiments and tests in the future.

Based on the result from the first year, we will conduct animal electrophysiology experiment with two-electrode and four-electrode virtual electrode scheme to study whether the four-electrode scheme is indeed better than the two-electrode scheme.

We will also assess the possibility of incorporating a proof of concept four electrode virtual channel human clinical trial since we already have experience in conducting a small human clinical trial based on two electrode virtual channel pitch ranking test (outside this NHRI project). This pitch ranking test identifies whether the CI patients are able to perceive virtual electrode and how many virtual electrode they can perceive.

According to this year's finding, we will assess the effect of stimulating strategies in terms of the local field potential responses recorded from the auditory cortex. Since we found activities of the gamma band power could reflect the tuning characteristics of the periphery inputs. We will implant with the electrode array into the auditory cortex and exploring the changes on the cortical responses. The benefit of this method can easily explore the cortical function in the behaving animals and we can evaluate the cochlear implantation for a longer duration. We will assess the responses of the cortical neurons before and after the deafen procedures as well as systemically evaluating effects of stimulating strategy at the 1st,

3rd, 5th, 7th, two weeks and one month after the cochlear implantation. The effects of the stimulating strategies will be assessed in terms of the tuning properties of the auditory neural responses and the long-term effects on the cortical connectivity. We will assess the effects of the stimulating strategies on the cochlear structures especially under the long-term stimulating condition.

六、 檢討與展望

From the engineering side, we will have developed a comprehensive 500~1000 channels stimulating strategy based on the four electrode virtual electrode scheme. We will study different variation of the stimulating strategy using N of M, or variation of the current stimulating strategies (but with 500~1000 channels resolution).

We will consider the possibility of conducting a small proof of concept human clinical trial using a 250~500 virtual channel stimulating strategy based on four electrodes current steering. If the CI patients can identify more distinct pitches using the four electrode scheme than with the two electrode scheme, then we have proven our concept is indeed better than the current CI technology.

We will study how to do cochlear implant mapping for the 500~1000 channel stimulating strategy based on the available CI maps of the CI patients. This will help us to transfer from the current technology to the new technology smoothly if the proposed four electrode current steering scheme works.

First, we will setup the ideal stimulating and recording system for the

future studies. For avoiding the interferences of the power line, we will consider to either apply the commercialized stimulating devices or to use the TDT system III stimulating and recording system (RZ5 and RA16 PA). Second, we will assess the effects of the stimulating strategies at least with 4-channel stimulating electrodes. Instead of using the handmade electrodes, we will purchased the commercialized stimulating electrode array (Cochlear, AU), which developed for the animal experiment. Therefore, we can reduce the variations on the electrode fabrication and put more efforts on the animal studies.

伍、97年度計畫所培訓之研究人員

註：群體/中心計畫者，不論是否提出各子計畫資料，都必須提出總計畫整合之資料

種類			人數	備註	
專任人員	1.	博士後研究人員	訓練中	0	
			已結訓	0	
	2.	碩士級研究人員	訓練中	3	
			已結訓	0	
	3.	學士級研究人員	訓練中	0	
			已結訓	0	
	4.	其他	訓練中	0	
			已結訓	0	
兼任人員	1.	博士班研究生	訓練中	1	
			已結訓	0	
	2.	碩士班研究生	訓練中	5	
			已結訓	0	
醫師		訓練中	0		
		已結訓	0		

特殊訓練課程（請於備註欄說明所訓練課程名稱）

陸、參與97年度計畫所有人力之職級分析

註：群體/中心計畫者，不論是否提出各子計畫資料，都必須提出總計畫整合之資料

職級	所含職級類別	參與人次
第一級	研究員、教授、主治醫師	2 人
第二級	副研究員、副教授、總醫師、助教授	1 人
第三級	助理研究員、講師、住院醫師	4 人
第四級	研究助理、助教、實習醫師	4 人
第五級	技術人員	4 人
第六級	支援人員	0 人
合計		15 人

〔註〕：

第一級：研究員、教授、主治醫師、簡任技正，若非以上職稱則相當於博士滿三年、碩士滿六年、或學士滿九年之研究經驗者。

第二級：副研究員、副教授、助研究員、助教授、總醫師、薦任技正，若非以上職稱則相當於博士、碩士滿三年、學士滿六年以上之研究經驗者。

第三級：助理研究員、講師、住院醫師、技士，若非以上職稱則相當於碩士、或學士滿三年以上之研究經驗者。

第四級：研究助理、助教、實習醫師，若非以上職稱則相當於學士、或專科滿三年以上之研究經驗者。

第五級：指目前在研究人員之監督下從事與研究發展有關之技術性工作，且具備下列資格之一者屬之：具初（國）中、高中（職）、大專以上畢業者，或專科畢業目前從事研究發展，經驗未滿三年者。

第六級：指在研究發展執行部門參與研究發展有關之事務性及雜項工作者，如人事、會計、秘書、事務人員及維修、機電人員等。

柒、參與97年度計畫所有人力之學歷分析

註：群體/中心計畫者，不論是否提出各子計畫資料，都必須提出總計畫整合之資料

類別	學歷別	參與人次
1	博士	3 人
2	碩士	4 人
3	學士	0 人
4	專科	0 人
5	博士班研究生	1 人
6	碩士班研究生	4 人
7	其他	4 人
	合計	16 人

捌、參與97年度計畫所有協同合作之研究室

註：群體/中心計畫者，不論是否提出各子計畫資料，都必須提出總計畫整合之資料

機構	研究室名稱	研究室負責人
國立成功大學醫學院生理學研究所		潘偉豐教授

玖、九十七年度計畫執行情形

註：群體計畫(PPG)者，不論是否提出各子計畫資料，都必須提出總計畫整合之資料

一、請簡述原計畫書中，九十七年預計達成之研究內容

First year

- Develop and set up a cochlear prosthesis research platform.
- Develop a simple test electrode for animal studies.
- Study and compare 2-electrode and 4-electrode current steering in electrical current spread experiments.
- Establish the implant procedures on the guinea pigs.
- Record the electrically evoked auditory brainstem response (EABR) from guinea pigs with cochlear implant and compare with that of normal guinea pigs.

二、請詳述九十七年度計畫執行情形，並評估是否已達到原預期目標（請註明達成率）

More than 90% of the tasks have been accomplished in the first year. One of the major reasons we are not able to finish all the tasks is because we were given the funding rather late. We did not receive funding until mid April to May. Since there is no electrophysiological recording laboratory at National Chiao Tung University, it takes us some time to set up the recording laboratory. Secondary, we were not able to hire the research assistants until after summer. All in all, we have accomplished what we targeted to do the first year.

A Develop and set up a cochlear prosthesis research platform.

We have completed the task we set in the proposal. The detail is described below.

A cochlear implant research platform has been set up (Fig. 1). A headpiece interface board was designed and implemented to interface with the commercial speech processor (PSP). The clinical programming interface (CPI) serves as an interface between the speech processor and the notebook computer. An oscilloscope is used to measure the output from the electric current source which is usually implanted in the human cochlea.

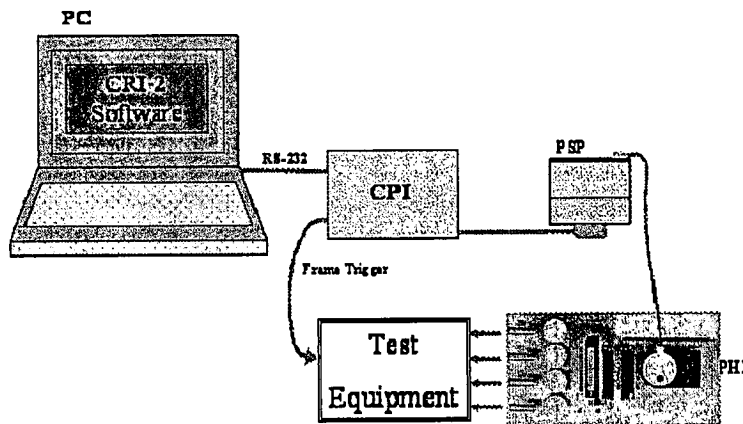


Fig. 1 Cochlear Implant Research Platform Setup. CPI stands for clinical programming interface; PSP is a speech processor; PHP is the headpiece and the implant receiver which is usually placed on the cochlear implant patient's head; the test equipment is an oscilloscope.

The output of the headpiece transmitted to the receiver (bottom unit in PHP in Fig. 1) and can be observed through an oscilloscope (Fig. 2). The output of the headpiece can be controlled by the notebook computer. Fig. 2 shows the output of the electrode contact which is linked to the implant receiver. Fig. 3 shows a typical biphasic sequence of pulses output by the implant current driver. Preliminary result shows that it is possible to control the output of the cochlear implant through the notebook computer via the speech processor. Since the speech processor internal architecture is unknown before the study, it takes a lot

of work to set up this research platform.

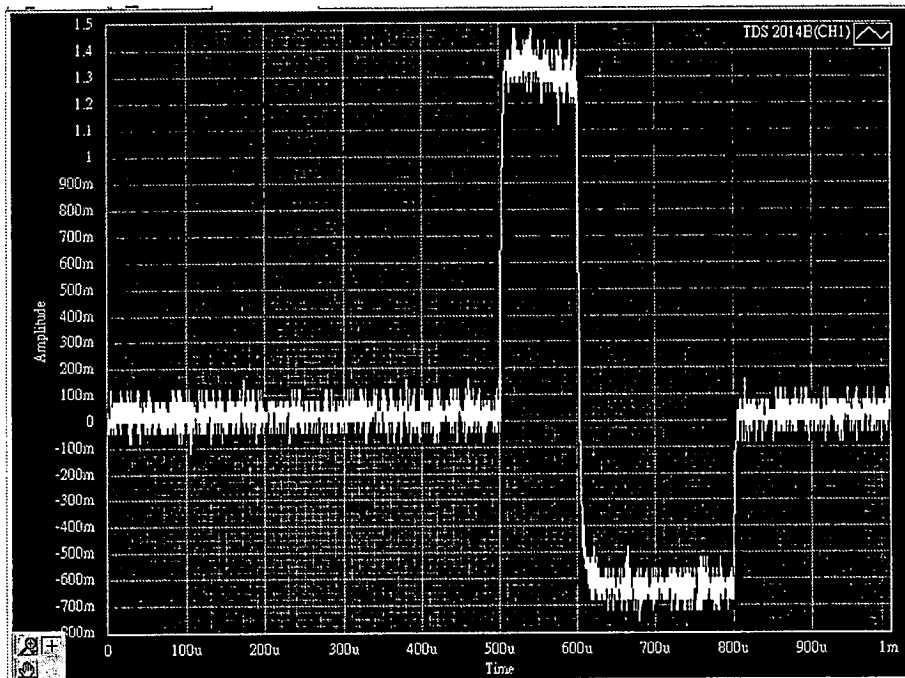


Fig. 2 The amplitude of positive phase is double to the amplitude of negative phase. The pulse width is opposite. The pulse width is 100µs and 1.4mA (1.4V with a 1Kohm terminal resistor) for the positive phase.

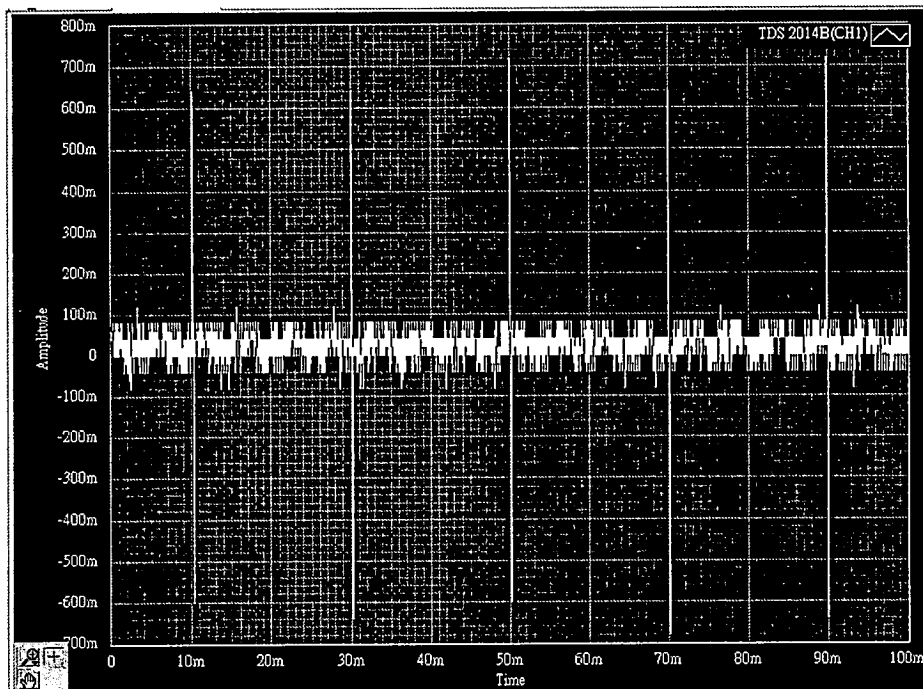


Fig. 3 This shows a typical biphasic pulse generated by the speech processor through the headpiece and the implant receiver.

B Study and compare 2-electrode and 4-electrode current steering in electrical current spread experiments.

We have accomplished what we aim to do in this project for the first year. This would be briefly described in the following paragraphs. The detailed will be described in the enclosed manuscript in the end of the report.

A half turn human cochlea model with a partial electrode array based on HiFocus-1j electrode array geometry from Advanced Bionics Corporation is used for study in this project (Fig. 4 and Fig. 5).¹ The cochlea model is constructed according to our early work,^{2,3,4,5} and is adapted to the dimension of scala tympani based on the study of Hatsuchika *et. al.*⁶ The modeled cochlea is embedded in a bone, which is not shown in the figure, to form the complete model. Although the structure of a real cochlea is spiral and tapering, the basal turn, especially for the first half turn, is close to a circular shape with a similar dimension. The modeled cochlea is applicable to approximate the examination of neural excitation pattern for simulation. The modeled electrode array is placed inside the scala tympani as a typical CI system. The four electrodes are embedded into an insulated carrier, ex. silicone rubber, and only the contact surfaces are exposed to the tissue. The spacing between each electrode contact is 1.1mm (center-to-center) and the dimension of each contact is 0.4mm in width and 0.3mm in height according to HiFocus-1j. The configuration of the electrode array is set to mono-polar and the central two electrode contacts (2nd and 3rd contacts of the electrode array) are used to generate virtual channels in this study. All the electrode contacts are organized to orient to the modiolus perpendicularly, as in general usage.

Fig. 6 show the activating function (AF) contour from the nerve fibers for the

electrode array located near the lateral wall at $d=0.9$ mm. The input current ratio α applied to the electrode pair is set to 50/50. According to the mechanism of electrical stimulation for nervous systems, the AF indicates the initial trans-membrane potential response of the nerve fiber; so the positive peak denotes the area of stimulation. Though the intermediate stimulation site can also be observed in the potential contour, AF is used to assess the virtual channel effect. The positive peak value of AF is normalized to 1×10^4 V/s for all α , which signifies an equal stimulation intensity to the nerve fiber. The squares below the x-axis denote the electrode contacts' position along the basilar membrane. An intermediate stimulation site between the electrode pair shown in the bottom of the Fig. 6 shows that this is a virtual channel since no physical electrode contact is positioned there. In order to effectively compare the virtual channels with the α , the AF at the nerve fiber node with a positive peak AF value along the basilar membrane is extracted, and the result forms the AF profile as shown in Fig. 7. From Fig. 7, five distinct virtual channels are generated which means that five different groups of nerve fibers are excited between the neighboring electrode contacts instead of the two generated in a typical stimulation strategy. For a four electrode current steering scheme, the AF contour shows that it is more focused than the case with two electrodes (Fig. 8).

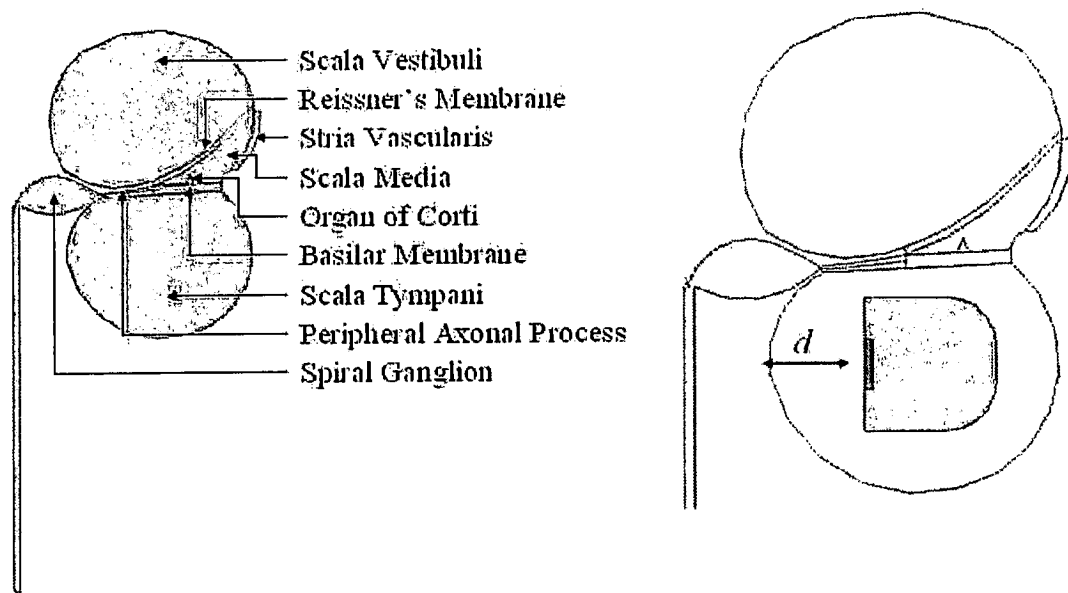


Fig. 4 shows the cross section diagram of a typical cochlea and electrode.

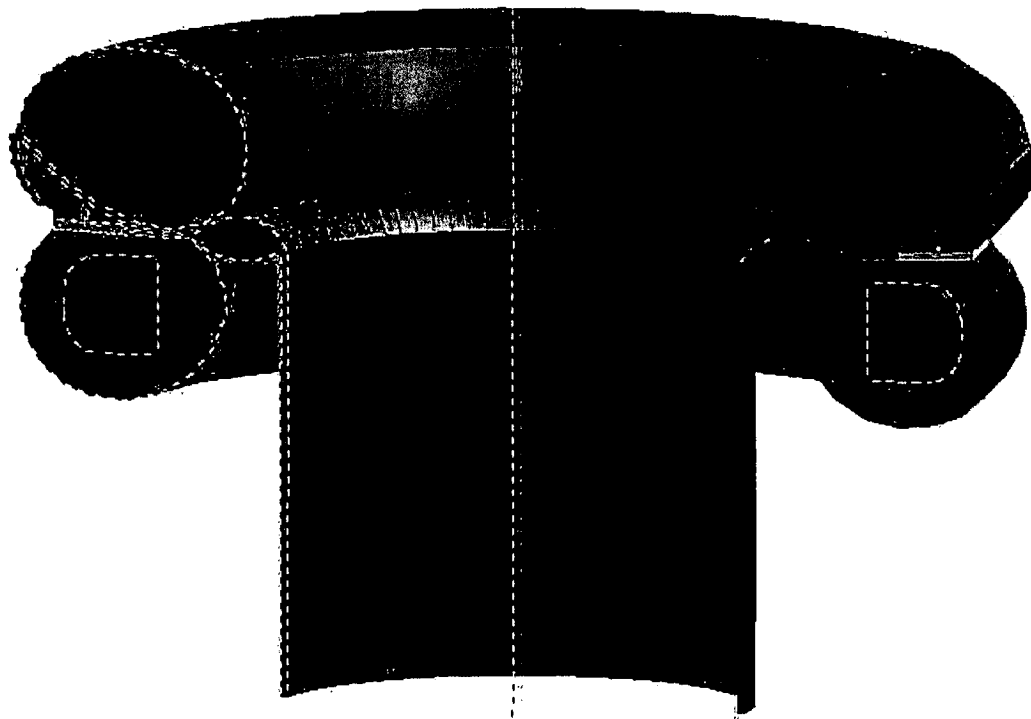


Fig. 5 This shows the half turn finite element model of the human cochlea.

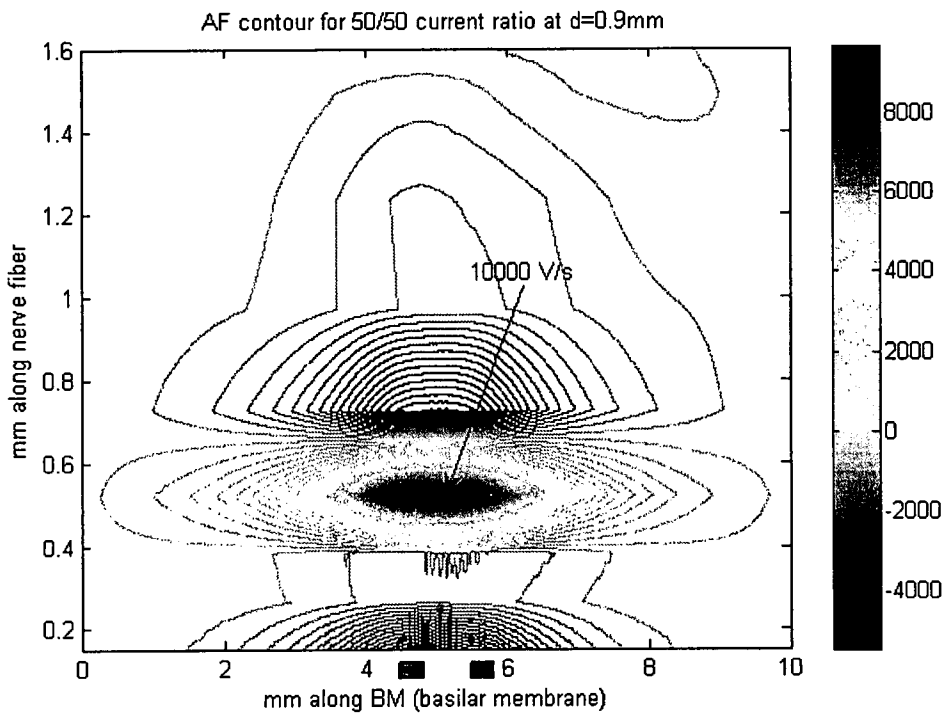


Fig. 6 This shows a activating function contour showing the location of the peak excitation of the auditory nerves in the cochlea. The inputs of the two electrodes (shown in red in the bottom of the Figure) are 50 and 50.

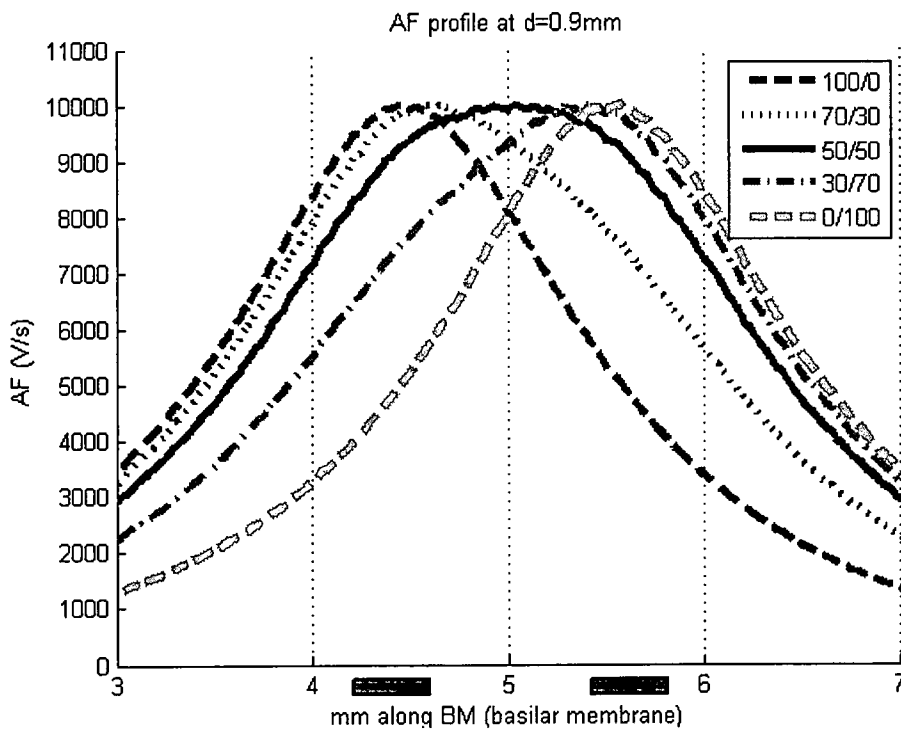


Fig. 7 shows a AF comparison of the 5 inputs. This shows the peak stimulation site can be steered according to the inputs.

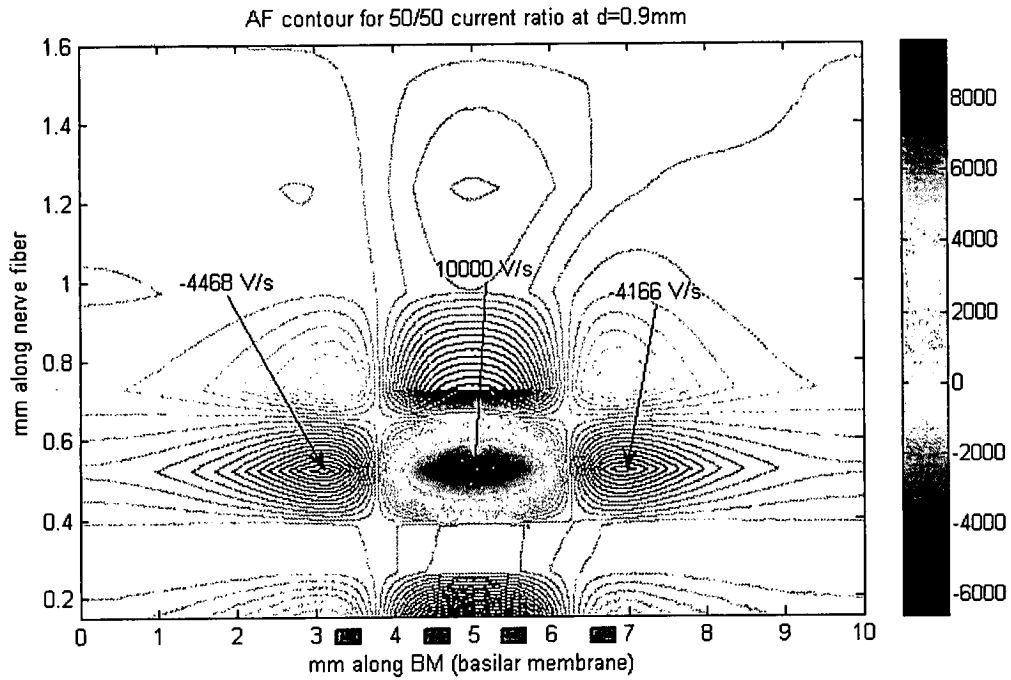


Fig. 8. The AF contour of four electrodes stimulation configuration for current ratio α equal to 0.5 (50/50) with type-1 form using HiFocus-1j electrode array. It can be seen that there are two negative peaks at the lateral side and that further limits the spreading of stimulation. The stimulation region is the narrowest in the three configurations.

C Establish the implant procedures on the guinea pigs. Record the electrically evoked auditory brainstem response (EABR) from guinea pigs with cochlear implant and compare with that of normal guinea pigs.

The aims of the first year is to setup the animal studies procedures including the ABR recording, the neomycin sulfate induced sensory hearing loss animal model the cochlear implant procedures and the electrical stimulating induced evoked potential recording system. Since there is no electrophysiological recording laboratory for in the NCTU, therefore we spent several months to setup a new laboratory for the electrophysiological recording. To successfully recording the auditory evoked responses from the guinea pig, we borrowed the TDT system II from Prof. P. Poon (one of our Co-PIs) to generate the auditory stimuli and recorded the evoked response from the auditory neurons. The detail procedures for the AEP recording and the results were shown in the following paragraph.

1. The AEP recoding procedures

A total of four albino guinea pigs (300 - 320g body weight) were implanted with subdural surface recording electrodes. Guinea pigs were anesthetized with an intra-peritoneal injection of urethane (Sigma, 1.8 g/kg). Supplementary doses were given at 10% of first dose whenever necessary as judged by the presence of pain withdraw reflex. An antiseptic solution (Povidine) was applied to the dorsal scalp surface before operation. The skull was then surgically exposed and connective tissue was removed with blunt dissection. After cleaning the skull surface with absolute ethanol, a dental drill was used to open two fenestrations (3 mm in diameter) on the skull. The dura was carefully removed for the insertion of electrodes. Customized bipolar electrodes made of Teflon-coated silver wires (WPI, 0.1 μ m OD) were connected to miniature strip sockets. In

order to record the auditory brainstem evoked potential (AEP) the active electrode was placed under the dura at the surface of the auditory cortex. Ground electrode was placed at the midline of frontal bone according to the AEP recording convention⁸. Figure 9 shows how electrodes we implanted on the skull during half way into surgery. An implanted electrode was fixed with dental cement (GC Fuji Plus, Tokyo). The resected skin closed with fine suture (6/0, Fig. 10). After surgery, animals were put in the recording table for electrophysiological recording. The recording electrodes with miniature socket connected through a flexible low-noise cable (New England Electric Wire Corp.) to a pre-amplifier (TDT system III, RA16LI). Signals were recorded, filtered (band pass filter between 100-3,000 Hz) and digitized by an analogue to digital converter (TDT system III, RA16 LI). AEP signals were captured at 16bits, 12 kHz sampling rate and stored into a computer (HP Pavilion a6635) for off-line analysis.



Figure 9: Picture showed positions of implanted electrode on a surgically prepared rat.

Acoustic stimuli was delivered to the animal inside a sound-treated room (1.5x1.5x2.5m³) through TDT electrostatic speaker (EC1 Electrostatic Speaker—Coupler Model). There were two kinds of stimuli were used in this experiment. Tone bursts of three different frequencies were used (1, 2 and 4 kHz, 2.5ms linear rise /fall time with a 15 ms plateau). Each single recording trial was

500 ms in duration with the stimulus onset at 25 ms.

Each stimulus session contained a total of 100 single trials during which the same stimulus was repeated at a fixed intensity. There was about a minute of interval between consecutive sessions. The pure tones were presented at the intensity of 75 dB. The traces of the evoked responses were further analyzed and presented in terms of the mean ERP and event-related spectral perturbation (ERSP).

The ERP results showed that the amplitude and the latency of the ERP responses were varied with the increase of the sound frequency. Specifically, the latency was decreased and the peak to peak amplitude was enhanced by the increment of the sound intensity (Fig. 10). In addition, we found that tone burst can induce a strong power increase at the gamma bands (30-180Hz) and the power increase was varied with the sound frequency. The strongest gamma band power was induced by the 4-kHz pure tone (Fig. 11). The results suggested that the gamma activities can be another index to assess the effect of the current steering on frequency resolution.

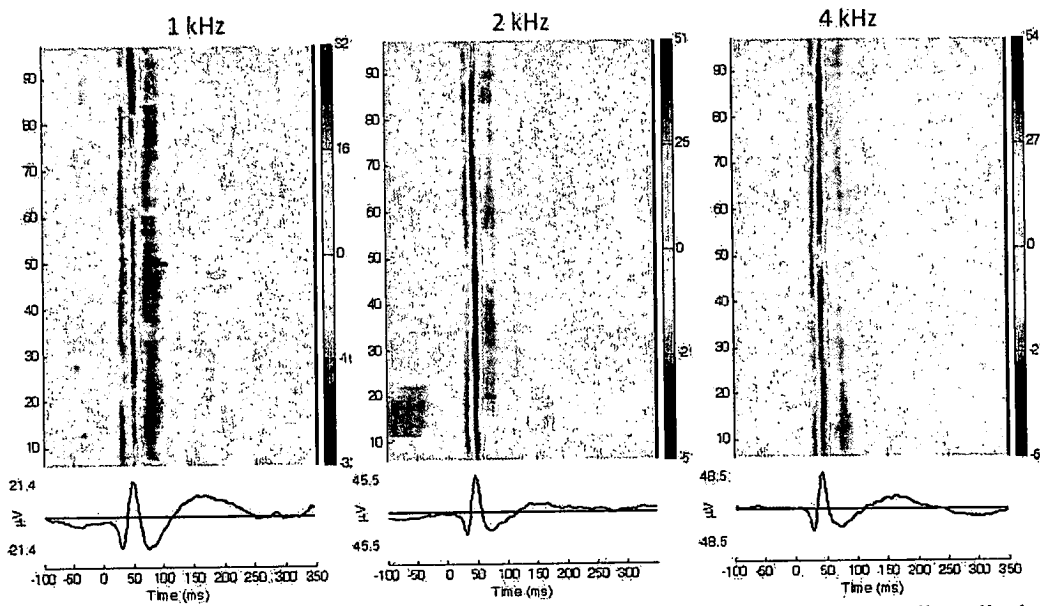


Figure 10: Pure tones stimuli in responses to AEP amplitude in pseudo-color coding display with different carrier frequencies (1, 2 and 4 kHz). The amplitude of the AEP was elevated by increases the carrier frequency from 1 kHz to 4 kHz). Color-coded of waveform amplitude was ranged from ± 21.4 to ± 48.5 (μV). Y-axis stood for number of trails. Post-stimulus onset time was displayed form -100 to 350 ms on x-axis. Zeros represented the onset time of sound transmitted to animal.

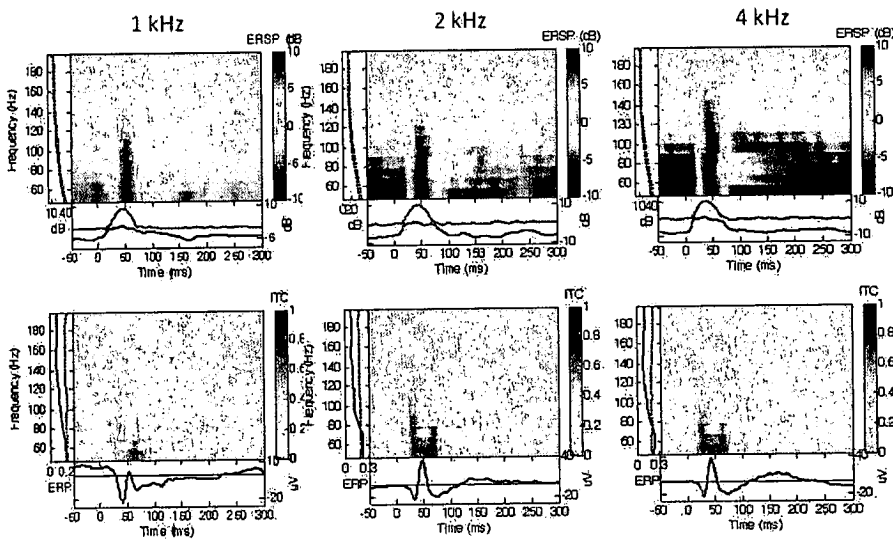


Figure 11: The above picture shows ERSP and inter-trial coherence (ITC) responses from auditory cortex from guinea pig when pure tone stimuli which are presented. Increases in gamma band activity (red) are found in increases the carrier frequency from 1 to 4 kHz. Post-stimulus onset time was displayed form -100 to 350 ms on x-axis. Zeros represented the onset time of sound transmitted to

animal.

2. Refine the configuration of the implanted electrodes

The stimulating contacts were fabricated by using Teflon insulated 0.001" diameter Pt:Ir (90:10) alloy wire was used to fabricate electrode arrays for acute experiments. The contacts were formed directly on Teflon insulated wire leads by melting an appropriate length of wire to form a sphere of desired size (100–150 μ m). This simple method reduces the possibility of lead breakage or corrosion that might occur with welds or mechanical connections between fine leads and more robust cables or dissimilar metals.

3. Setup the procedures of the cochlea implantation

A total of 2 animals were included for the deafening procedures and the cochlea implantation. The left bulla was accessed using a post-auricular approach. Deafening was achieved by puncture of the round window, withdrawal of a small amount of perilymph with a wick, then slow infusion of 60 μ l of 10% neomycin sulfate (approximately 0.1 M) into the scala tympani, around 2 h after the neomycin infusion and the beginning of brain stem evoked potential recording. Deafness was confirmed by monitoring the evoked response up to a level of 105 dB (Fig. 12 and Fig. 13). The intracochlear electrode array was inserted into scala tympani through a cochleostomy approximately 1 mm beyond the round window and a ground electrode was positioned in a neck muscle. The stimulating electrodes with miniature socket connected through a flexible low-noise cable (New England Electric Wire Corp.) to the stimulator.

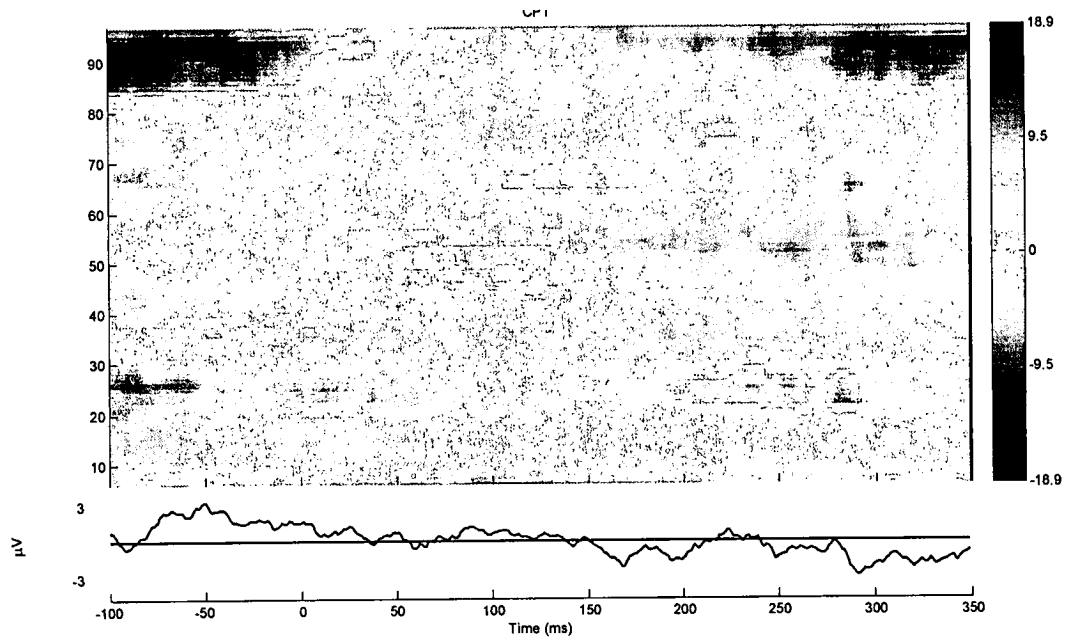


Figure 12: Pure tones stimuli in responses to AEP amplitude in pseudo-color coding display with 4 kHz and 105 dB. No apparent evoked responses were found after the neomycin sulfate injected. Color-coded of waveform amplitude was ranged from $\pm 3 \mu\text{V}$. Y-axis stood for number of trails. Post-stimulus onset time was displayed form -100 to 350 ms on x-axis. Zeros represented the onset time of sound transmitted to animal.

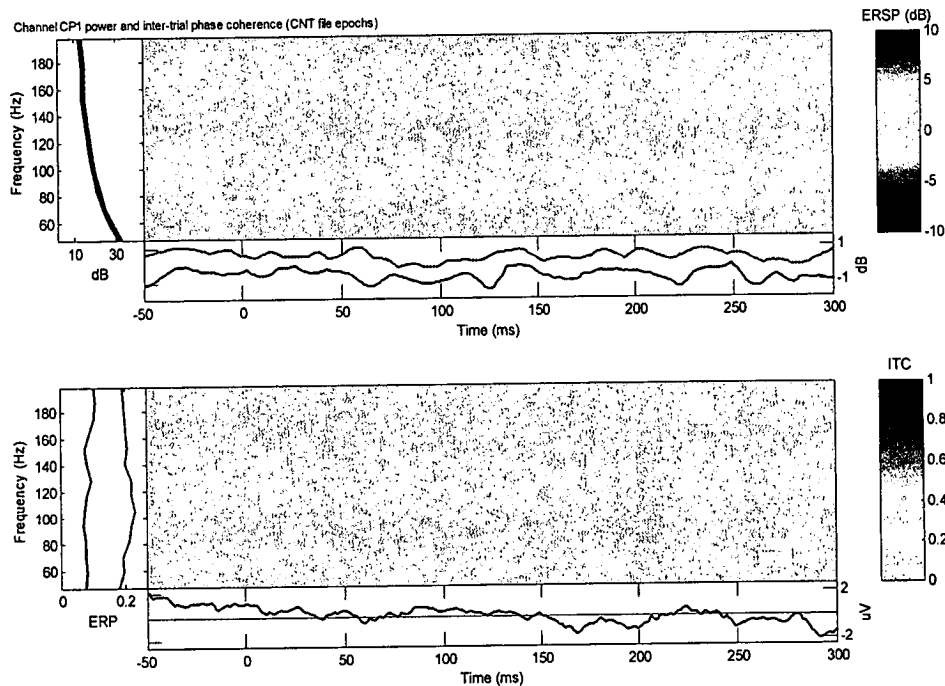


Figure 13: The ERSP and ITC responses from auditory cortex from guinea pig when the 4 kHz, 105 dB pure tone stimuli are presented. No apparent gamma band activities are found after infusion with the 10% neomycin sulfate.

4. Test the possibility of the simultaneous stimulating and recording electrodes

The stimuli were two symmetric biphasic current pulses, 200 μ s per pulse, delivered with 50 ms inter-pulse interval. The activating cathodic current was applied to the first intra-cochlear electrode and the second intra-cochlear electrode provided the return current path. Two stimulation intensities (500 μ A and 1.6 mA) were chosen for the testing. The electrical evoked brainstem potentials were recorded from -200ms to 200ms after the stimulation. Since the electrical stimulation was given from the testing board which was with the power line, the recording signals were contaminated with the 60 Hz. We will setup another new TDT system in the middle of December which can sent the

electrical stimuli and recorded the electrical stimuli simultaneously without the contaminated with power line. We will use this new stimulating and recording system for the further study.

REFERENCES

- ¹ Advanced Bionics Corporation. HiRes 90K: surgeon's manual for the HiFocus Helix and HiFocus lj electrodes. 2005
- ² Advanced Bionics Corporation. Increasing spectral channels through current steering in HiResolution bionics ear users. 2005
- ³ Choi, C.T.M., W.D. Lai, and Y.B. Chen. Optimization of cochlear implant electrode array using genetic algorithms and computational neuroscience models. *IEEE Trans. Magn.* 40(2):639-642, 2004.
- ⁴ Choi, C.T.M., W.D. Lai, and Y.B. Chen. Comparison of the electrical stimulation performance of four cochlear implant electrodes. *IEEE Trans. Magn.* 41(5):1920-1923, 2005.
- ⁵ Choi, C.T.M. and W.D. Lai. Modeling the virtual channels of the cochlear implant systems. Proceedings of the IEEE Conference on Electromagnetic Field Computation (CEFC 2006), Miami, Florida, USA, 2006.
- ⁶ Choi, C.T.M. and C.H. Hsu. Models of virtual channels based on various electrode shape. Proceedings of the 6th Asia Pacific Symposium on Cochlear Implants and Related Sciences, Sydney, 2007.
- ⁷ Hatsuchika, S, R.K. Shepherd, Y.C. Tong, G.M. Clark, Funasaka S. Dimensions of the scala tympani in the human and cat with reference to cochlear implants. *Ann. Otol. Rhinol. Laryngol.* 99(11): 871-876, 1990.
- ⁸ Shaw NA, A possible collicular component of the auditory evoked potential and its relationship to brainstem and cerebellar auditory potentials. *Electromyogr Clin Neurophysiol.* 32(12):579-90, 1992.

拾、附錄

無

拾壹、本年度之著作抽印本或手稿

Editorial Manager(tm) for Annals of Biomedical Engineering
Manuscript Draft

Manuscript Number: ABME1772R1

Title: Conditions for Generating Virtual Channels in Cochlear Prosthesis Systems

Article Type: Research Article

Keywords: Cochlear prosthesis, cochlear implant, virtual channel, current steering, electrical stimulation, volume conduction model, activating function, finite element analysis

Corresponding Author: Dr. Charles T. M. Choi, PhD

Corresponding Author's Institution: National Chiao Tung University

First Author: Charles T. M. Choi, PhD

Order of Authors: Charles T. M. Choi, PhD; Chien-Hua Hsu, MS

Abstract: Simultaneous electrical stimulation of neighboring electrodes in cochlear prosthesis systems generates channel interaction. However, intermediate channels, or virtual channels between the neighboring electrodes can be created through controlled channel interaction. This effect may be exploited for sending new information to the hearing nerves by stimulating in a suitable manner. The actual stimulation sites are therefore not limited to the number of electrodes. Clinical experiments, however, show that virtual channels are not always perceived. In this paper, electrical simulation with finite element analysis on a half turn human cochlea model is adopted to model the virtual channel effect, and the conditions for generating virtual channels are discussed. Five input current ratios (100/0, 70/30, 50/50, 30/70, 0/100) are applied to generate virtual channels. Three electrode array parameters are taken into consideration: distance between electrode contact and modiolus, spacing between adjacent electrode contacts and scale of electrode contact size. By observing the activating function contours, the virtual channel patterns and performances can be measured and examined. The results showed that a broad excitation pattern is necessary to produce the kind of electrode interaction that can form distinct virtual channels.

1
2
3
4
5
6 **Conditions for Generating Virtual Channels in Cochlear**
7
8 **Prosthesis Systems**
9

10
11
12 Charles T. M. Choi and Chien-Hua Hsu
13

14
15
16 Department of Computer Science and Institute of Biomedical Engineering
17

18
19 National Chiao Tung University, Hsin Chu, Taiwan, R.O.C.
20
21

22
23
24
25 Running head: Conditions for Generating Virtual Channels
26

27
28 Correspondence: Charles T. M. Choi, PhD
29

30
31 Department of Computer Science and Institute of Biomedical Engineering
32

33
34 National Chiao Tung University
35

36
37 1001 Ta Hsueh Road, Hsinchu, Taiwan 300, R.O.C.
38

39
40 Phone: +886-3-573-1978, Fax: +886-3-572-1490
41

42
43 c.t.choi@ieee.org
44
45
46
47
48
49
50
51
52
53
54
55
56
57
58
59
60
61
62
63
64
65

1
2
3
4
5 **Abstract**—Simultaneous electrical stimulation of neighboring electrodes in cochlear prosthesis
6
7
8 systems generates channel interaction. However, intermediate channels, or virtual channels
9
10 between the neighboring electrodes can be created through controlled channel interaction. This
11
12 effect may be exploited for sending new information to the hearing nerves by stimulating in a
13
14 suitable manner. The actual stimulation sites are therefore not limited to the number of
15
16 electrodes. Clinical experiments, however, show that virtual channels are not always perceived.
17
18
19 In this paper, electrical simulation with finite element analysis on a half turn human cochlea
20
21
22 model is adopted to model the virtual channel effect, and the conditions for generating virtual
23
24 channels are discussed. Five input current ratios (100/0, 70/30, 50/50, 30/70, 0/100) are applied
25
26 to generate virtual channels. Three electrode arrays parameters are taken into consideration:
27
28 distance between electrode contact and modiolus, spacing between adjacent electrode contacts
29
30 and scale of electrode contact size. By observing the activating function contours, the virtual
31
32 channel patterns and performances can be measured and examined. The results showed that a
33
34 broad excitation pattern is necessary to produce the kind of electrode interaction that can form
35
36 distinct virtual channels.
37
38
39
40
41
42
43
44
45
46
47
48

49 ***Index Terms*** – Cochlear prosthesis, cochlear implant, virtual channel, current steering,
50
51
52 electrical stimulation, volume conduction model, activating function, finite element analysis
53
54
55
56
57
58
59
60
61
62
63
64
65

I. INTRODUCTION

Cochlear implant (CI) technology has been developed for years to help people with profound hearing impairment to recover partial hearing. Typically, sound is captured by a microphone and is fed into a signal processor. The signal processor breaks the input signal into different frequency bands or channels and delivers the filtered signal to drive electrodes which are used to stimulate auditory nerve fibers.^{14,20} The number of spectral bands of stimulation is determined by the number of electrodes. Currently, there are only about 12~22 electrodes implanted into a CI user for a commercially available device while there are about 30,000 or more auditory nerve fibers for a typical human ear. The lack of spectral resolution due to the small number of electrode can contribute to poor speech perception in noise, music perception, and tonal language understanding.²⁵

For speech processing strategies, electrical stimulation by two electrodes can produce two pitch components, but channel interactions are generated by stimulating individual electrodes simultaneously,³ which produce threshold changes consistent with instantaneous electric field summation. This will affect or distort the intended perception and usually is undesirable. However, experiments show that by exciting two adjacent electrodes simultaneously in a suitable manner,^{2,10,15,17,22,23,24} the CI users can perceive a pitch which is between two pitches perceived when the two electrodes are excited individually. The intermediate pitch is the so called virtual channel since there is no real electrode to generate a real stimulation channel there. The mechanism for controlling the virtual channels, called current steering,^{2,10,15,22} steers the current applied to adjacent electrodes in

1
2
3
4
5 order to generate virtual channels according to the current ratio between the electrodes. This technique
6
7
8 can be used to expand the spectral resolution without changing the implanted hardware or the number
9
10
11 of CI electrodes.
12
13

14 The virtual channel can also be simulated by a modeling approach with the result being consistent
15
16 with the experiment result.^{4,7} In our early work,⁸ virtual channel effect based on the finite element
17
18 model with different electrode contact shape, was studied. In the study, planar, ball and half band
19
20 electrode contacts were modeled, which covered the most popular design of electrode arrays then and
21
22 now. The result showed that the examined shapes can create virtual channels normally; any difference
23
24 in the effect due to the shape was not apparent.
25
26
27
28
29
30

31 In clinical experiments, however, virtual channels are not always perceived,^{2,10,15,22,23,24} perhaps due
32
33 to the individual hearing loss factor of each user or improper electrical stimulation from the electrodes.
34
35 From the experiment results, it is found that virtual channels at the medial and apical electrode pairs
36
37 are easier to perceive.^{10,15} Since the medial and apical electrodes are usually closer to the lateral wall
38
39 of the cochlea, thus generating a larger current spread and more channel interaction.²¹ Clinical
40
41 experiments show the possibility that the generation of virtual channels by electrical stimulation could
42
43 be linked to the distance between the electrode contacts and the auditory nerves (modiolus).
44
45
46
47
48
49
50
51

52 Generally, the current design of the electrode array tends to decrease the channel interaction in
53
54 order to provide the improved stimulation efficacy of individual electrodes, such as moving the
55
56 electrode array closer to the modiolus (Contour array of CochlearTM and Hifocus-helix array of
57
58
59
60
61
62
63
64
65

1
2
3
4 Advanced Bionics Corporation) or enlarging the distance between adjacent electrode contacts (Medel
5
6
7 C40+ array). However, since the virtual channel depends upon a suitable electrical interaction, the
8
9
10 interaction free design mechanism might decrease the effect of the virtual channel and thus may affect
11
12
13 the outcome of the clinical experiments. In this paper, a finite element model incorporating various
14
15
16 electrode array configurations is used to study the conditions for generating virtual channels and to
17
18
19 assess the virtual channel's effect in cochlear prosthesis systems. Although neural survival
20
21
22 distribution has significant impact on the creation of virtual channels, it is beyond the scope of this
23
24
25 paper and will be addressed in future studies.
26
27

28 29 30 **II. METHODS**

31 32 33 *A. Model of the Human Cochlea and Analysis Approach*

34
35
36 A half turn human cochlea model with a partial electrode array based on HiFocus-1j electrode array
37
38
39 geometry from Advanced Bionics Corporation is used for study in this paper (Fig. 1 and Fig. 2).¹ The
40
41
42 cochlea model is constructed according to our early work,⁵ and is adapted to the dimension of scala
43
44
45 tympani based on the study of Hatsuchika *et. al.*¹² The modeled cochlea is embedded in a bone, which
46
47
48 is not shown in the figure, to form the complete model. Although the structure of a real cochlea is
49
50
51 spiral and tapering, the basal turn, especially for the first half turn, is close to a circular shape with a
52
53
54 similar dimension. The modeled cochlea is applicable to approximate the examination of neural
55
56
57 excitation pattern for simulation. The modeled electrode array is placed inside the scala tympani (Fig.
58
59
60 3) as a typical CI system. The four electrodes are embedded into an insulated carrier, ex. silicone
61
62
63
64
65

1
2
3
4
5 rubber, and only the contact surfaces are exposed to the tissue. The spacing between each electrode
6
7
8 contact is 1.1mm (center-to-center) and the dimension of each contact is 0.4mm in width and 0.3mm
9
10
11 in height according to HiFocus-1j. The configuration of the electrode array is set to mono-polar and
12
13 the central two electrode contacts (2nd and 3rd contacts of the electrode array) are used to generate
14
15
16 virtual channels in this study. All the electrode contacts are organized to orient to the modiolus
17
18
19 perpendicularly, as in general usage.
20
21

22
23 The finite element method is used to compute the potential distribution in the human cochlea
24
25 model.⁵ The resulting mesh of the model shown in Fig. 4 contains 97,197 nodes and 554,192
26
27
28 tetrahedra. The material resistivity parameters used in this model are listed in Table I.^{6,11} The
29
30
31 electrical potential from the nerve fiber model is extracted in order to calculate the activating function
32
33
34 (AF) along the basilar membrane and nerve fiber.^{6,11,18,19} The AF is the forcing term in the
35
36
37 Hodgkin-Huxley equation which calculates the variation of trans-membrane potential and determines
38
39
40 the excitation for a nerve fiber. As a result, the initial trans-membrane potential response of the nerve
41
42
43 fiber is proportional to the AF value. The result of the finite element model can be used to plot an AF
44
45
46 contour which provides a global view for locating the virtual channel and evaluating its
47
48
49 performance.^{6,11} Since AF is computed based on static electric potential, it cannot be used to
50
51
52 investigate the effect of stimulation rate and stimulation pulse width. The effect of stimulation rate
53
54
55 and stimulation pulse width have on virtual channel will be addressed in another study. Neural
56
57
58 refractoriness¹⁶ and spike rate adaptation can produce temporal interaction in virtual channels, but this
59
60
61
62
63
64
65

1
2
3
4 is beyond the scope of this paper and will also be addressed another study.
5
6

7
8 *B. Configurations of the Electrode Array*
9

10
11 Three electrode array parameters are examined for this study: distance between electrode contact
12 and modiolus, spacing between adjacent electrode contacts and the scale of the electrode contact size.
13
14 To examine the virtual channels, the electrical signals to be interacted are in phase. A ratio α of the
15
16 input current is applied to the adjacent electrode pair and is normalized to five cases: 100/0, 70/30,
17
18 50/50, 30/70, 0/100, which theoretically means that five distinct virtual channels can be generated.
19
20
21
22
23
24

25
26 *1) Distance between Electrode Contact and Modiolus:* In the first simulation, the electrode array is
27
28 placed at locations with various distances d (0.9 ~ 0.4mm) from the inner wall of the scala tympani
29
30 (Fig. 1). The range is adjusted according to the dimension and shape of both the electrode array and
31
32 the scala tympani so that they fit each other well. Due to the large size of the electrode carrier which
33
34 occupies the space near the outer region of the scala tympani, the positions of the electrode contacts
35
36 are distributed in the medial and inner regions of the scala tympani. Generally, the exact position of
37
38 the implant electrode array is not easily controlled and is different for each CI user after the electrode
39
40 array insertion surgery. Typically, it is best to place the electrode array very close to the modiolus in
41
42 order to provide a higher stimulation efficacy, a lower electrical interaction and an improved
43
44 stimulation power. However, there is no study which examines the relationship with regard to the
45
46 virtual channel effect and the distance of electrode contacts to the modiolus. This simulation aims to
47
48 study this kind of configuration.
49
50
51
52
53
54
55
56
57
58
59
60
61
62
63
64
65

1
2
3
4
5 2) *Spacing between Adjacent Electrode Contacts*: The second simulation is to examine the
6
7 relationship with regard to the virtual channel effect and the spacing between adjacent electrode
8
9 contacts. Due to the inertia and stress for the carrier of Hifocus-1j, the electrode array usually lies
10
11 against the lateral wall. The electrode array is therefore placed at the outer region of the scala tympani
12
13 ($d = 0.8\text{mm}$) for this study. Various spacing s ($0.8 \sim 1.3\text{mm}$, center-to-center) between adjacent
14
15 electrode contacts which covers most of novel design of electrode array, ex. Hifocus-Helix, is
16
17 organized to study the effect of this parameter (Fig. 3).
18
19
20
21
22
23
24

25 3) *Scale of Electrode Contact Size*: The study of this situation can be separated into two factors:
26
27 height h and width w of the electrode contact (Fig. 3) with only one factor varied at a time. The
28
29 electrode array is located at the outer region of the scala tympani ($d = 0.8 \text{ mm}$) as the consideration
30
31 above shows. The spacing between adjacent electrode contacts is fixed at 1.1 mm (center-to-center).
32
33
34 Due to the typical dimension of the scala tympani and the electrode array, the height h varies in the
35
36 range of $0.1 \sim 0.5 \text{ mm}$ with the width ranging from $0.1 \sim 0.6 \text{ mm}$.
37
38
39
40
41
42
43

44 III. RESULTS

45
46
47 In order to provide an efficient assessment of the virtual channel effect, several factors are
48
49 examined. An AF contour provides an impression of the excitation pattern for the electrical
50
51 stimulation and an AF profile extracted from an AF contour provides a comparison virtual channel
52
53 pattern for the five cases of α . Virtual channel positions, beam widths and the total current provide
54
55 systematic comparisons; the details are illustrated in the following paragraph.
56
57
58
59
60
61
62
63
64
65

1
2
3
4
5 Fig. 5 and Fig. 6 show the potential and the activating function (AF) contour from the nerve fibers
6
7
8 for the electrode array located near the lateral wall at $d=0.9$ mm. The input current ratio α applied to
9
10 the electrode pair is set to 50/50. According to the mechanism of electrical stimulation for nervous
11
12 systems,^{18,19} the AF indicates the initial trans-membrane potential response of the nerve fiber; so the
13
14 positive peak denotes the area of stimulation. Though the intermediate stimulation site can also be
15
16 observed in the potential contour, AF is used to assess the virtual channel effect. The positive peak
17
18 value of AF is normalized to 1×10^4 V/s for all α , which signifies an equal stimulation intensity to the
19
20 nerve fiber. The squares below the x-axis denote the electrode contacts' position along the basilar
21
22 membrane. An intermediate stimulation site between the electrode pair shown in the bottom of the Fig.
23
24 6 shows that this is a virtual channel since no physical electrode contact is positioned there. In order to
25
26 effectively compare the virtual channels with the α , the AF at the nerve fiber node with a positive
27
28 peak AF value along the basilar membrane is extracted, and the result forms the AF profile as shown
29
30 in Fig. 7. From Fig. 7, five distinct virtual channels are generated which means that five different
31
32 groups of nerve fibers are excited between the neighboring electrode contacts instead of the two
33
34 generated in a typical stimulation strategy.
35
36
37
38
39
40
41
42
43
44
45
46
47
48
49

50 However, virtual channels are not always generated or easily distinguishable in locations of
51
52 different distances d from the simulation result. Fig. 8 shows the AF contour for the electrode array
53
54 located near the inner wall with $d=0.4$ mm. Two stimulation peaks appear corresponding to the
55
56 positions of the two active electrodes along the basilar membrane. This result is undesirable since it
57
58
59
60
61
62
63
64
65

1
2
3
4 does not generate only one distinct virtual channel. The AF profile in Fig. 9 shows the five generated
5
6
7
8 virtual channels tend to spread to the lateral sites which are the locations of the real electrode contacts.
9
10
11 This makes the virtual channels indistinguishable.

12
13 By examining the distances d (Fig. 10), it is found that when the electrode array is placed toward
14
15
16 the lateral wall of the scala tympani ($d=0.7\sim 0.9\text{mm}$), the virtual channels generated are more
17
18
19 distinctive and the further the electrode array is from the modiolus, the more distinct the virtual
20
21
22 channels are. When the electrode array is placed toward the inner wall of the scala tympani
23
24
25 ($d=0.4\sim 0.6\text{mm}$), the generated virtual channels are indistinguishable; the closer the electrode array to
26
27
28 the modiolus is, the less distinct the virtual channels are. This result is consistent with the modeling
29
30
31 result from Briaire *et al.*⁴
32

33
34 Fig. 11 provides the systematic comparison of the virtual channel effect for the different locations
35
36
37 of the electrode array. Fig. 11(a) shows the virtual channel position vs. the input current ratio α . The
38
39
40 virtual channel position is defined as the geometric center for the positive peak in the AF profile. It
41
42
43 provides a view for distinguishing different virtual channels. It can be seen that when the electrode
44
45
46 array is located near the lateral wall, the virtual channels varied more consistently with α (near linear
47
48
49 distribution). However, when the electrode array is located near the inner wall, the virtual channels
50
51
52 are hardly distinguishable and are distributed to the sites where the real electrode contacts reside. The
53
54
55 linearity of the virtual channel position distribution is important since it provides simplicity for
56
57
58 controlling the virtual channel positions with the input current ratio.
59
60
61
62
63
64
65

1
2
3
4 Fig. 11(b) shows the virtual channel beam width vs. the input current ratio α . For the sake of
5
6
7
8 simplicity, the virtual channel beam width is defined as the width of the AF profile at the half power
9
10
11 level along the basilar membrane. Though the actual beam width depends on the neural firing
12
13 threshold, this can also enable a theoretical analysis. Typically, it is found that the narrower the beam
14
15 width is, the more concentrated the virtual channels are. It is narrower for the virtual channels near the
16
17 real electrode contacts since the stimulation there has better spatial selectivity. It can be observed that
18
19 the virtual channel beam width is narrower for the electrode array located near the inner wall than
20
21 when the array is near the lateral wall, since it is more concentrated when the electrode contact
22
23 approaches the modiolus. It is the opposite for the intermediate channel due to the difficulty in
24
25 generating virtual channels for the electrode array when located near the modiolus. Besides, the beam
26
27 width is more uniform for all virtual channels when the electrode array is located near the lateral wall,
28
29 in comparison to the higher variation of beam width when the array is located near the inner wall.
30
31 Uniformity of beam width can provide a similar stimulation range for all virtual channels for CI users
32
33 to perceive uniformly.
34
35
36
37
38
39
40
41
42
43
44
45

46 Fig. 11(c) shows the total input current vs. the input current ratio α . The total input current is input
47
48 to bring the positive peak AF to the normalized value, ie. 1×10^4 V/s, for all cases. The result shows
49
50 that when the electrode array was placed near the lateral wall, the total current is higher since the
51
52 current spreads out, which makes for inefficient stimulation to the nerve fibers. It can also be observed
53
54 that the virtual channels near the center position need a higher current than do those near the real
55
56
57
58
59
60
61
62
63
64
65

1
2
3
4 electrode contacts. Therefore, the intermediate channels need higher input current in order to generate
5
6
7 equal electrical stimulation intensity. This is comparable to the modeling result from Litvak et. al.¹³
8
9

10 The spacing between adjacent electrode contacts is another factor which influences the virtual
11
12 channel effect. Fig. 12 shows the AF profiles of all the examined spacing s for the electrode array
13
14 located at the outer region ($d=0.8$ mm). It can be observed that when s is shorter, the virtual channels
15
16 generated are more distinctive, but not so if it is wider. As the distance between electrode contact and
17
18 the modiolus decreases, and the closer the adjacent electrode contacts (center-to-center), the more
19
20 distinct the virtual channels are. In observing the channel position, beam width and total input current
21
22 in Fig. 13, the comparison is more apparent. The channel position distribution is more linear and the
23
24 beam width is more uniform and narrower when s is shorter. The total current required is also smaller
25
26 for shorter s since more current interacts with closer electrode contacts to generate effective electrical
27
28 stimulation.
29
30
31
32
33
34
35
36
37
38
39

40 For the simulation of the scale of electrode contact size, it is found that the relation between the
41
42 virtual channel effect and scale of the electrode contact size is insignificant. This can be observed
43
44 from Fig. 14(a), (b) and Fig. 15(a), (b) for height and width examination. The channel position and
45
46 beam width in the figures almost overlap and are indistinguishable. The AF profiles are all very
47
48 similar and therefore are not shown here. The only influence is the total input current. Fig. 14(c) and
49
50 Fig. 15(c) shows the total input current applied to the smaller electrodes is lower than that applied to
51
52 the larger ones, but the difference is not apparent.
53
54
55
56
57
58
59
60
61
62
63
64
65

IV. DISCUSSION

This paper explored the conditions for generating virtual channels and assessed the virtual channel effect for various configurations of electrode arrays in cochlear prosthesis systems. The modeling approach and numerical analysis allowed us to study comprehensive conditions which are not achieved easily in clinical experiments or animal studies. The results provide a systematic view for virtual channels. The adoption of the dimension of an actual electrode array (ex. Hifocus-1j) made the study more accurate and realistic.

A. Clinical Experiment and Electrode Array Location

Generally, it is better to have an electrode array with a large number of electrode contacts and place them very close to the modiolus. This can improve the spatial selectivity of stimulation and reduce channel interaction. It is possible to increase the effective number of electrode by adding virtual channels or virtual electrodes to the real electrodes, i.e. the physical number of electrode contacts. Since virtual channel depends on the electrical interaction of the stimulation and the efficacy of the stimulation, consequently, the degree of electrical interaction can affect the quality and the number of virtual channels generated. From the simulation results, the farther the electrode array is from the modiolus, the poorer the spatial selectivity and the better the results will be regarding the generation of more distinct virtual channels via electrical stimulation. This is consistent with the discussion on the cause of virtual channels, which showed that the virtual channels require suitable

1
2
3
4 interaction between neighboring electrodes. More distinct virtual channels mean that the CI
5
6
7 users can effectively perceive more number of channels, which is the goal of all auditory
8
9
10 prostheses.
11

12
13 Due to the mismatch in size, curvature and shape of the electrode array inside the cochlea in
14
15 different individual CI users, the spiral trajectory usually causes the electrode array to lie against the
16
17 lateral wall of the cochlea, especially at the medial and apical parts. From the clinical experiment
18
19 results,^{2,10,15,22} there are more distinct and perceptible virtual channels at the medial and apical
20
21 electrode pairs than those at the basal electrode pair. Although those experiments did not provide data
22
23 on where the electrode array is located, if the electrode array is indeed located closer to the lateral
24
25 wall in the medial and apical parts, this is in consistent with our modeling result.
26
27
28
29
30
31
32

33 34 *B. Electrical Potential Distribution and Interaction*

35
36 Typically, the spacing between electrode contacts is designed wide enough to prevent electrical
37
38 interaction. However, from the electrical point of view, the potential distribution is inversely
39
40 proportional to the distance. The power is mainly distributed around the electrical source, i.e. the
41
42 electrode contact, and decays rapidly as the distance increases. When two electrode contacts are
43
44 spaced far apart, the potential contributed by the two electrode contact between the two electrode
45
46 contacts will be less due to the larger distance. On the other hand, when two electrode contacts are
47
48 spaced close enough, the potential from the two electrode contacts can interact to generate an
49
50 intermediate channel which is the so-called virtual channel. From the simulation result, the effect of
51
52
53
54
55
56
57
58
59
60
61
62
63
64
65

1
2
3
4
5 the virtual channels is not apparent when the spacing between electrode contacts is further apart, but it
6
7
8 does improve the virtual channel performance when the spacing is closer.
9

10 11 V. CONCLUSION

12
13
14 A modeling approach with finite element analysis is proposed to study the conditions for generating
15
16
17 virtual channels. The modeling result provides several directions for the electrode design to improve
18
19
20 the virtual channels. First, the farther the electrode contacts are from the modiolus, it will be easier to
21
22
23 produce the kind of electrode interaction that can form distinctive virtual channel. Second, the closer
24
25
26 the adjacent electrode contacts are, the stronger the electrical interaction creating more of the virtual
27
28
29 channel effect. The dimensions of the electrode contact have small impact on the virtual channels
30
31
32 generation. All these simulation results can be used as reference and electrode design rules for
33
34
35 future studies on virtual channels.
36
37
38

39 40 VI. ACKNOWLEDGMENTS

41
42
43 This research was supported in part by the National Science Council of the Republic of China
44
45
46 under contract number: NSC95-2221-E-009-366-MY3 and National Health Research Institute of
47
48
49 Republic of China under grant: NHRI-EX97-9735EI.
50
51
52
53
54
55
56
57
58
59
60
61
62
63
64
65

1
2
3
4
5
6 REFERENCES
7
8

- 9 ¹ Advanced Bionics Corporation. HiRes 90K: surgeon's manual for the HiFocus Helix and HiFocus
10
11
12 1j electrodes. 2005
13
14
15 ² Advanced Bionics Corporation. Increasing spectral channels through current steering in
16
17
18 HiResolution bionics ear users. 2005
19
20
21 ³ Balthasar, C., C. Boex, G. Cosendai, G. Valentini, A. Sigrist, M. Pelizzone. Channel interactions
22
23
24 with high-rate biphasic electrical stimulation in cochlear implant subjects. *Hearing Res.* 182:77-87,
25
26
27 2003.
28
29
30 ⁴ Briaire, J., R. Kalkman, J. Frijns. Current steering: new model insights. Poster presented at the
31
32
33 Proceedings of the 9th International Conference on Cochlear Implants, Vienna, Austria, 2006.
34
35
36 ⁵ Choi, C.T.M., W.D. Lai, and Y.B. Chen. Optimization of cochlear implant electrode array using
37
38
39 genetic algorithms and computational neuroscience models. *IEEE Trans. Magn.* 40(2):639-642,
40
41
42 2004.
43
44
45 ⁶ Choi. C.T.M., W.D. Lai, and Y.B. Chen. Comparison of the electrical stimulation performance of
46
47
48 four cochlear implant electrodes. *IEEE Trans. Magn.* 41(5):1920-1923, 2005.
49
50
51 ⁷ Choi, C.T.M. and W.D. Lai. Modeling the virtual channels of the cochlear implant systems.
52
53
54 Proceedings of the IEEE Conference on Electromagnetic Field Computation (CEFC 2006), Miami,
55
56
57 Florida, USA, 2006.
58
59
60
61
62
63
64
65

- 1
2
3
4
5⁸ Choi, C.T.M. and C.H. Hsu. Models of virtual channels based on various electrode shape.
6
7
8 Proceedings of the 6th Asia Pacific Symposium on Cochlear Implants and Related Sciences, Sydney,
9
10 2007.
11
12
13
14⁹ Donaldson, G.S., H.A. Krefth, L. Litvak. Place-pitch discrimination of single- versus dual-electrode
15
16 stimuli by cochlear implant users. *J. Acoust. Soc. Am.* 118(2):623-626, 2005
17
18
19
20¹⁰ Firszt, J.B., Koch, D.B. Downing, Litvat. Current steering creates additional pitch percepts in adult
21
22 cochlear implant recipients. *Otol. and Neurotol.* 28:629-636, 2007.
23
24
25
26¹¹ Hanekom, T. Three-dimensional spiraling finite element model of the electrically stimulated
27
28 cochlea. *Ear and Hearing.* 22:300-315, 2001.
29
30
31
32¹² Hatsuchika, S, R.K. Shepherd, Y.C. Tong, G.M. Clark, Funasaka S. Dimensions of the scala
33
34 tympani in the human and cat with reference to cochlear implants. *Ann. Otol. Rhinol. Laryngol.*
35
36 99(11): 871-876, 1990.
37
38
39
40
41¹³ Litvak, L.M., J. Anthony, Spahr, E. Gulam. Loudness growth observed under partially tripolar
42
43 stimulation: model and data from cochlear implant listeners. *J. Acoust. Soc. Am.* 122(2):967-981,
44
45 2007.
46
47
48
49
50¹⁴ Loizou, P. Mimicking the human ear. *IEEE Signal Process. Mag.* 15(5):101-130, 1998.
51
52
53
54
55
56
57
58
59
60
61
62
63
64
65¹⁵ Luk, B.P.K., T.K.C. Wong, M.C.F. Tong. Increasing spectral bands using current steering in
66
67 cochlear implant users. Proceedings of the 6th Asia Pacific Symposium on Cochlear Implants and
68
69 Related Sciences, Sydney, 2007.

- 1
2
3
4
5
6
7
8
9
10
11
12
13
14
15
16
17
18
19
20
21
22
23
24
25
26
27
28
29
30
31
32
33
34
35
36
37
38
39
40
41
42
43
44
45
46
47
48
49
50
51
52
53
54
55
56
57
58
59
60
61
62
63
64
65
- ¹⁶ Mino, Hiroyuki and J. T. Rubinstein, Effects of Neural Refractoriness on Spatio-Temporal Variability in Spike Initiations with Electrical Stimulation, *IEEE Trans. Neural Sys. Rehab. Eng.* 14(3):273-280, 2006.
- ¹⁷ Oguz, P. and P.C. Loizou. Pitch perception using virtual channels. Proceedings of the Conference on Implantable Auditory Prostheses, Asilomar, Monterey, CA, 2001.
- ¹⁸ Rattay, F. Analysis of models for extracellular fiber stimulation. *IEEE Trans. Biomed. Eng.* 36(7):676-682, 1989.
- ¹⁹ Rattay, F. The basic mechanism for the electrical stimulation of the nervous system. *Neuroscience.* 89(2):335-346, 1999.
- ²⁰ Spelman, F.A. The past, present, and future of cochlear prostheses. *IEEE Eng. Med. Biol.* 18(3):27-33, 1999.
- ²¹ Stickney, G., P. C. Loizou, L. N. Mishra, P. F. Assmann, R. V. Shannon, J. M. Opie. Effects of electrode design and configuration on channel interactions. *Hearing Res.* 211:33-45, 2006.
- ²² Trautwein, P., 2006. HiRes with fidelity 120 sound processing: implementing active current steering for increased spectral resolution in CII BionicEar ® and HiRes90K users. Advanced Bionics Corporation, Valencia, CA.
- ²³ Townsend B., N. Cotter, D. Van Compernelle, R. L. White. Pitch perception by cochlear implant subjects. *J. Acoust. Soc. Am.* 82(1):106015, 1987.

1
2
3
4
5
6
7
8
9
10
11
12
13
14
15
16
17
18
19
20
21
22
23
24
25
26
27
28
29
30
31
32
33
34
35
36
37
38
39
40
41
42
43
44
45
46
47
48
49
50
51
52
53
54
55
56
57
58
59
60
61
62
63
64
65

²⁴ Wilson, B. S. and M. F. Dorman. Cochlear implants: current design and future possibilities. J. Rehabil. Res. Dev. 45(5):695-730, 2008.

²⁵ Zeng, F. G., K. Nie, G. S. Stickney, Y. Y. Kong, M. Vongphoe, A. Bhargave, C. Wei, K. Cao. Speech recognition with amplitude and frequency modulations. Proc. Natl. Acad. Sci. U.S.A., 102(7):2293-8, Feb. 15 2005.

1
2
3
4
5
6
7
8
9
10
11
12
13
14
15
16
17
18
19
20
21
22
23
24
25
26
27
28
29
30
31
32
33
34
35
36
37
38
39
40
41
42
43
44
45
46
47
48
49
50
51
52
53
54
55
56
57
58
59
60
61
62
63
64
65

TABLE I
MATERIAL PROPERTIES FOR COCHLEA AND ELECTRODE MODELS

Model component	Resistivity ($\Omega \cdot m$)
Electrode metal	0.001
Scala tympani and vestibuli	0.7
Scala media	0.6
Bone	6.41
Spiral ganglion	3
Peripheral axonal process (anisotropic)	3 (axial) 15 (transverse)
Reissner's membrane	340.13
Basilar membrane	4
Stria vascularis	125.79
Organ of Corti	83.333

1
2
3
4 Fig. 1. Cross-section of the cochlea model studied. The electrode array is located at a position of
5
6 distance d between the electrode contact surface and the inner wall of the scala tympani.
7
8

9
10 Fig. 2. The finite element model of the cochlear implant system.
11
12

13 Fig. 3. The electrode array of the cochlear implant model. The electrode contacts are spacing with
14
15 various s (center-to-center). The dimension of the electrode contact: height h and width w .
16
17
18

19 Fig. 4. Mesh of the modeled cochlea which contains 97197 nodes and 554192 tetrahedra.
20
21

22 Fig. 5. The Potential contour for electrode array located against the lateral wall with $d=0.9\text{mm}$. The
23
24 squares below the x-axis denote the contacts position. The negative peak point (-0.318V) is indicated
25
26 by the arrow.
27
28
29

30 Fig. 6. The AF contour for HiFocus-1j electrode array located against the lateral wall with $d=0.9\text{mm}$
31
32 and current ratio α equal to 0.5 (50/50). The squares below the x-axis denote the contacts position.
33
34
35

36 Fig. 7. The AF profile of two electrodes stimulation configuration for the five cases of input current
37
38 ratio α using HiFocus-1j electrode array.
39
40
41

42 Fig. 8. The AF contour for electrode array located near the inner wall with $d=0.4\text{mm}$. There are two
43
44 peaks indicating there are two sites of maximum stimulation.
45
46
47

48 Fig. 9. The AF profile for the five cases of input voltage ratio α .
49
50

51 Fig. 10. The AF profiles for all of the examined distances d ($0.4 \sim 0.9 \text{ mm}$).
52
53

54 Fig. 11. The comparison of the AF profiles for all of the examined distances d ($0.4 \sim 0.9 \text{ mm}$). (a) VC
55
56 center position vs. α (b) VC beam width vs. α (c) VC current vs. α .
57
58
59
60
61
62
63
64
65

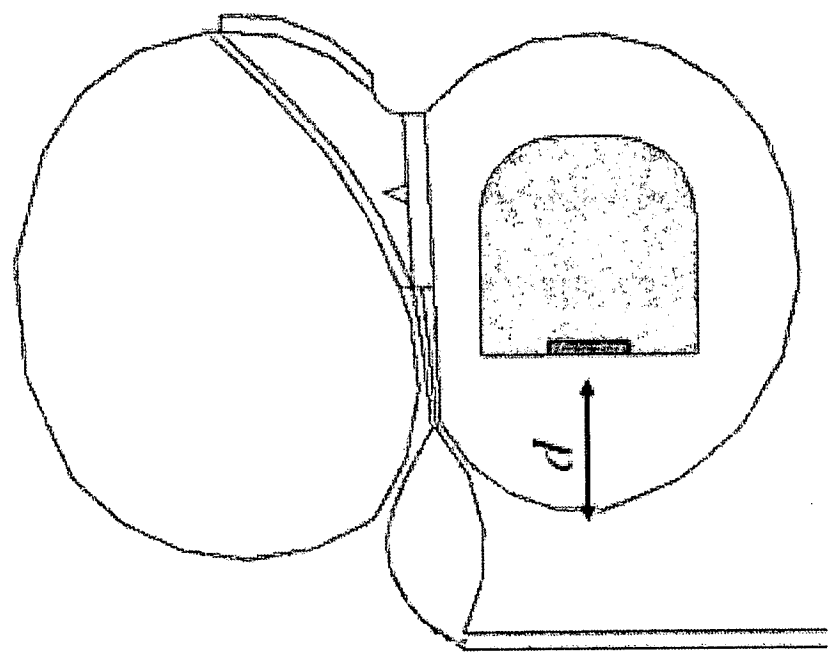
1
2
3
4
5 Fig. 12. The AF profiles for all of the examined spacing s (0.8 ~ 1.3 mm). The electrode array is
6
7 located at outer region of scala tympani ($d = 0.8$ mm).
8
9

10
11 Fig. 13. The comparison of the AF profiles for all of the examined spacing s (0.8 ~ 1.3 mm). (a) VC
12
13 center position vs. alpha (b) VC beam width vs. alpha (c) VC current vs. alpha. The electrode array is
14
15 located at outer region of scala tympani ($d = 0.8$ mm).
16
17
18

19
20 Fig. 14. The comparison of the AF profiles for all of the examined height h (0.1 ~ 0.5 mm). (a) VC
21
22 center position vs. alpha (b) VC beam width vs. alpha (c) VC current vs. alpha. The electrode array is
23
24 located at outer region of scala tympani ($d = 0.8$ mm).
25
26
27

28
29 Fig. 15. The comparison of the AF profiles for all of the examined width w (0.1 ~ 0.6 mm). (a) VC
30
31 center position vs. alpha (b) VC beam width vs. alpha (c) VC current vs. alpha. The electrode array is
32
33 located at outer region of scala tympani ($d = 0.8$ mm).
34
35
36
37
38
39
40
41
42
43
44
45
46
47
48
49
50
51
52
53
54
55
56
57
58
59
60
61
62
63
64
65

Figure 1
Click here to download high resolution image



- Scala Vestibuli
- Reissner's Membrane
- Stria Vascularis
- Scala Media
- Organ of Corti
- Basilar Membrane
- Scala Tympani
- Peripheral Axonal Process
- Spiral Ganglion

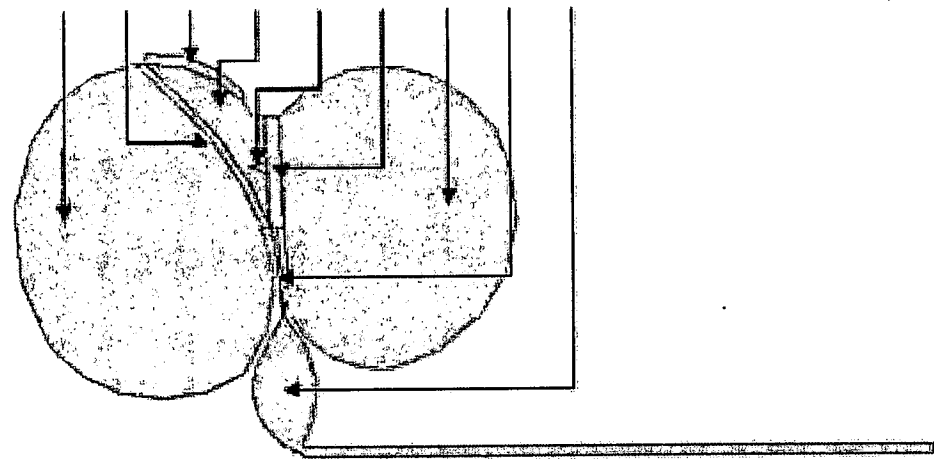


Figure 2
[Click here to download high resolution image](#)

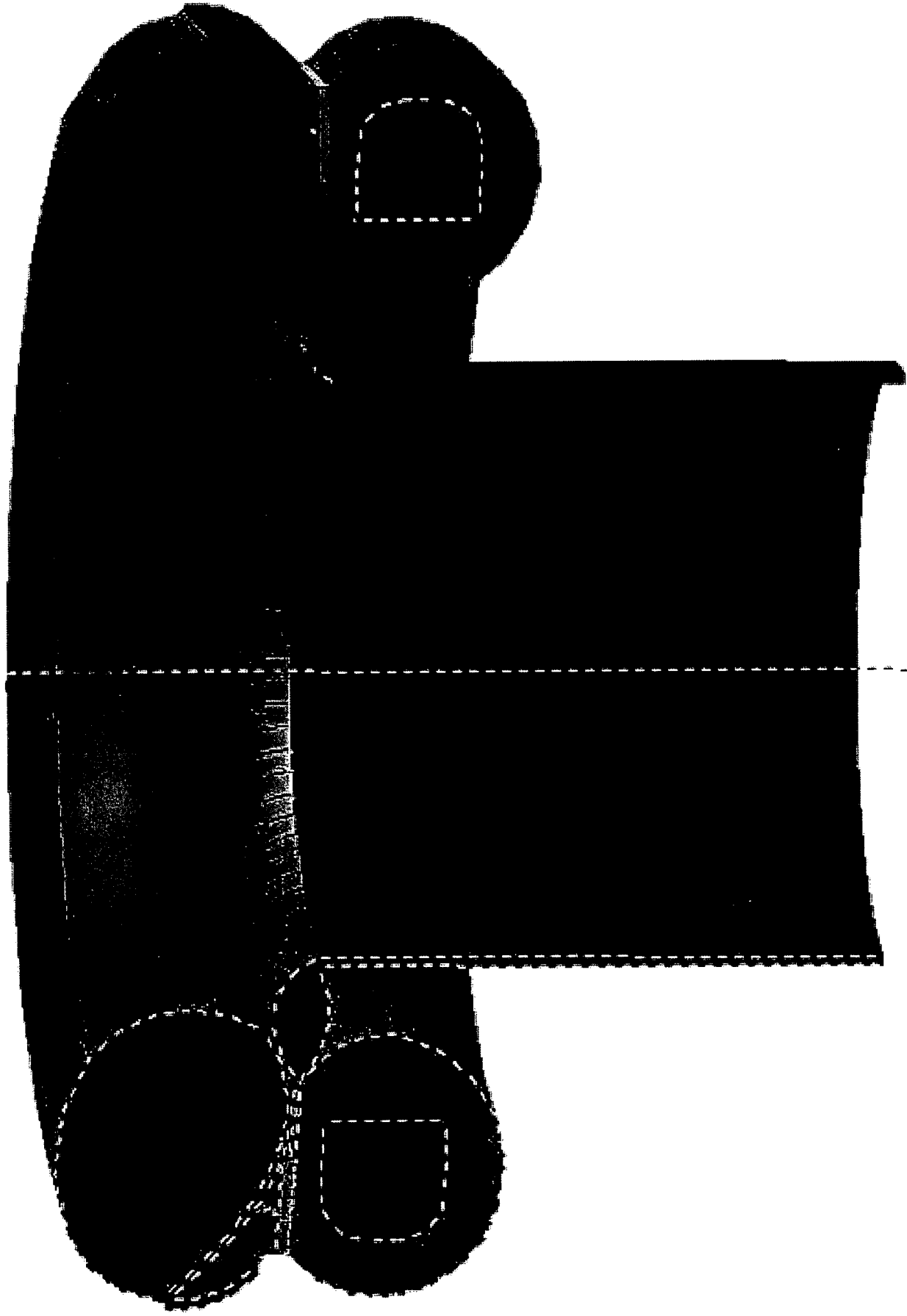


Figure 3
[Click here to download high resolution image](#)

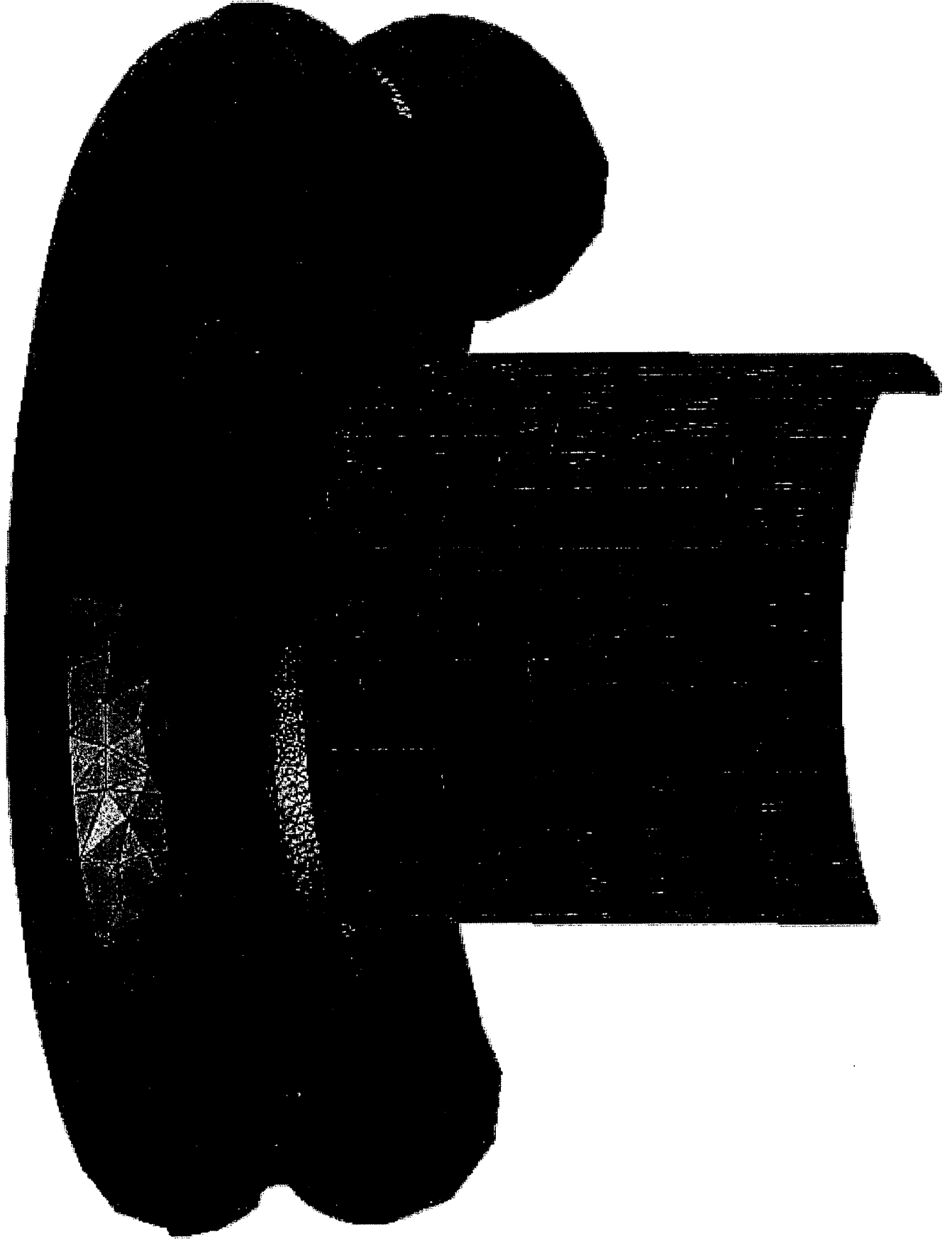


Figure 4
Click here to download high resolution image

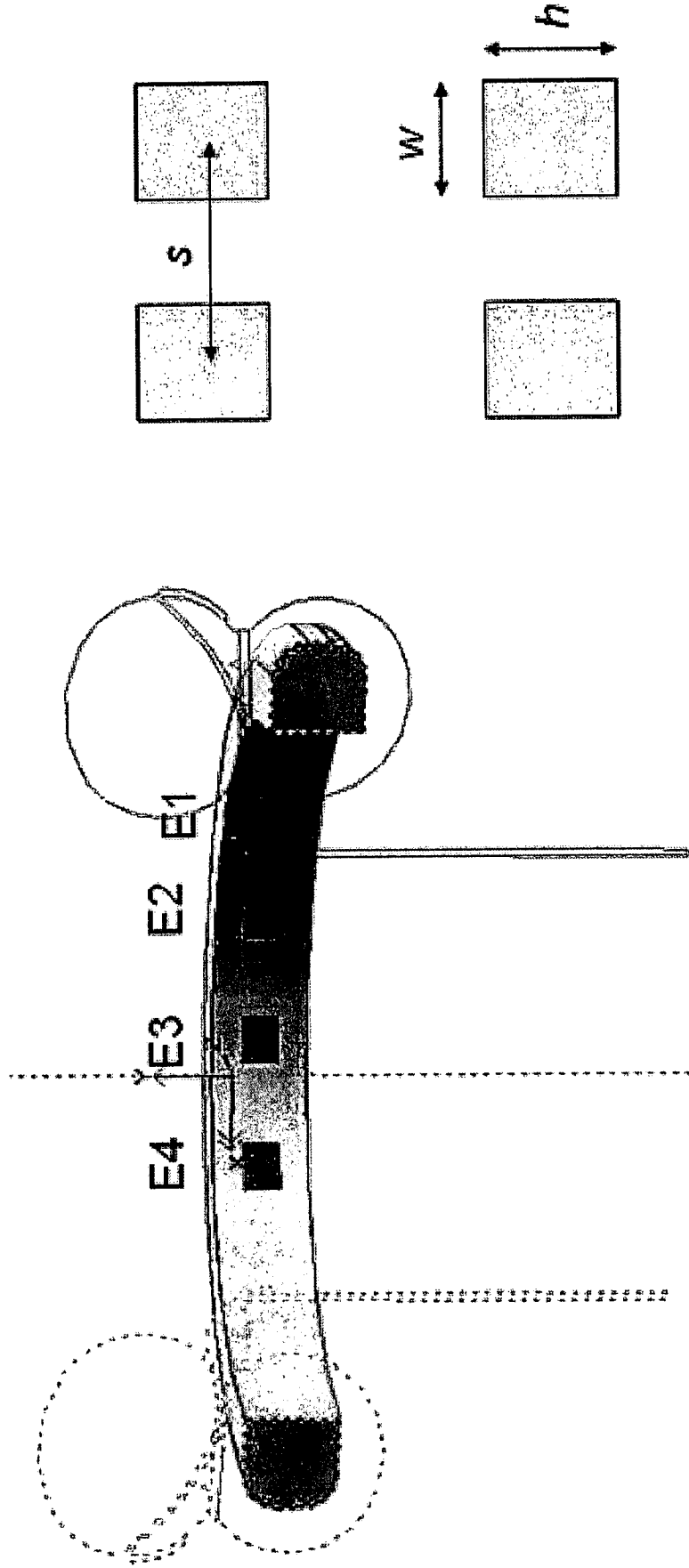


Figure 5
Click here to download high resolution image

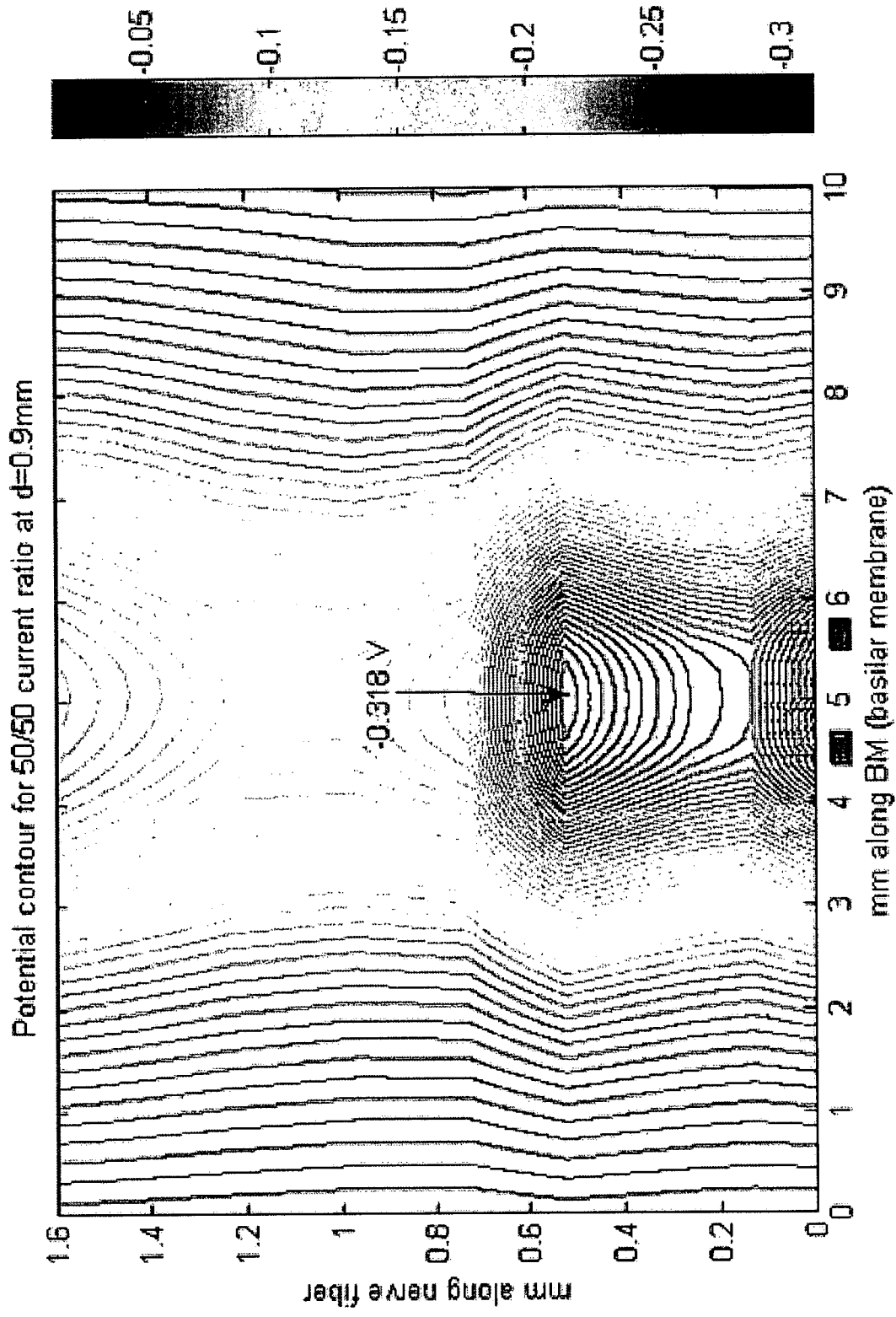
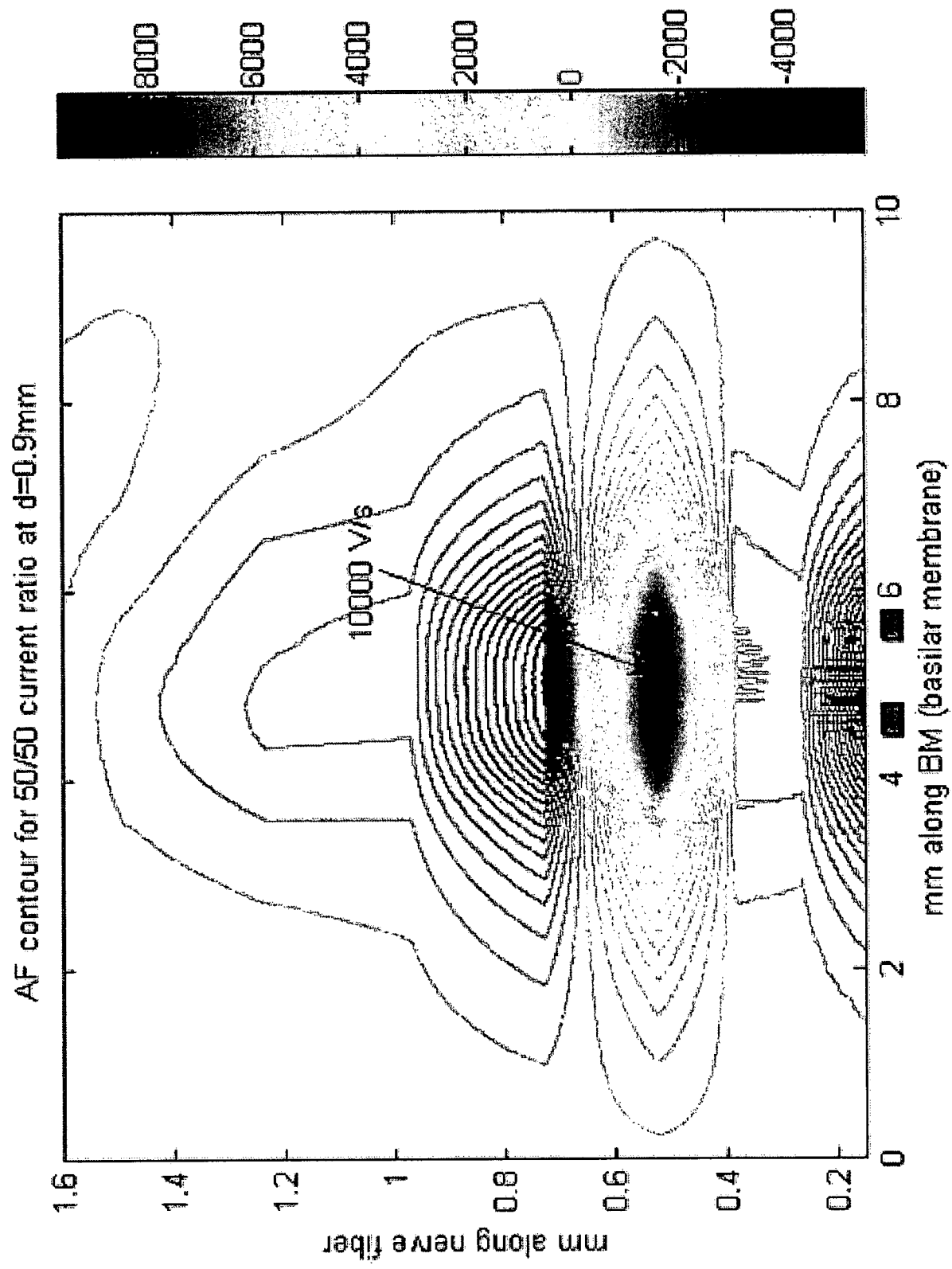


Figure 6
Click here to download high resolution image



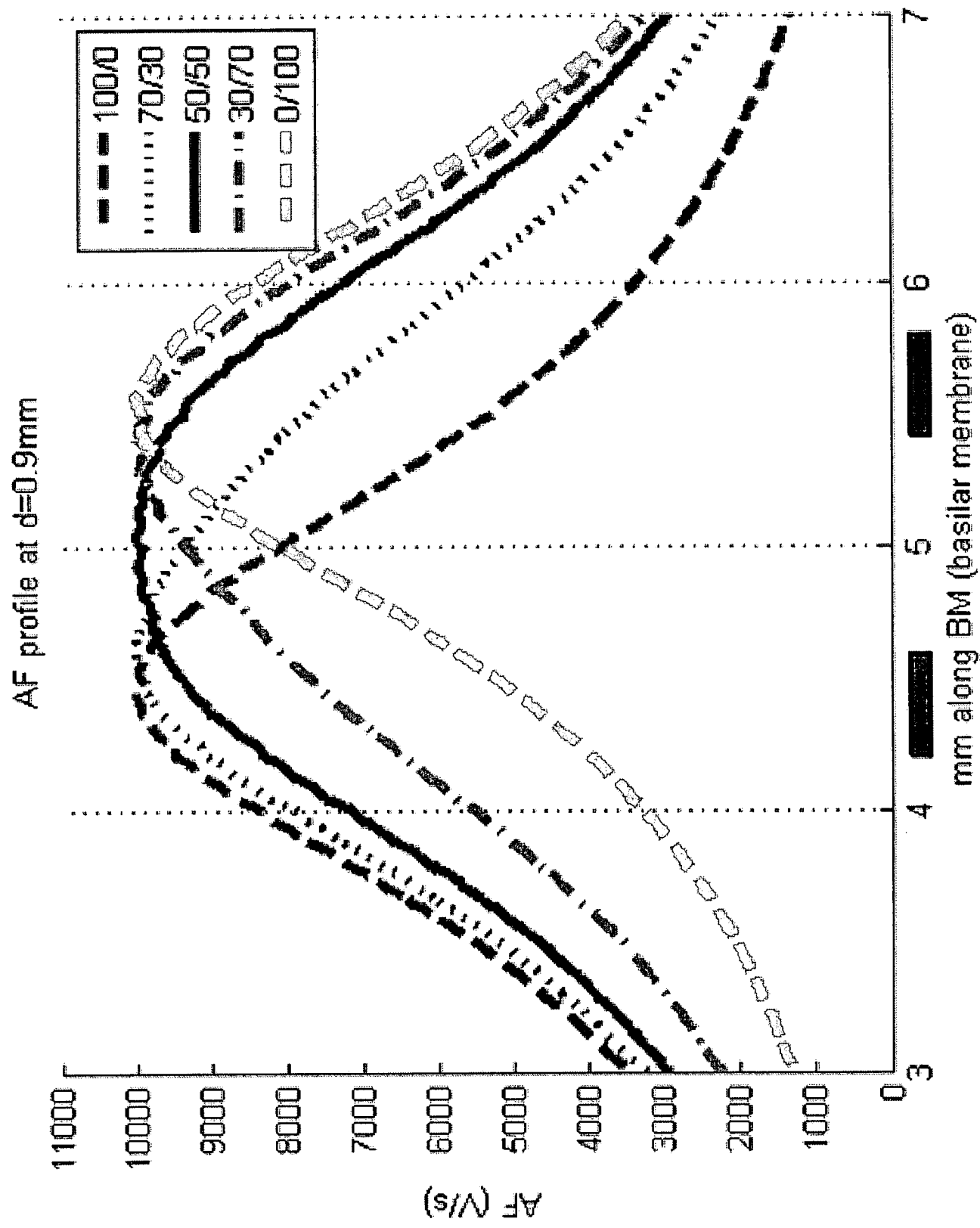


Figure 8
Click here to download high resolution image

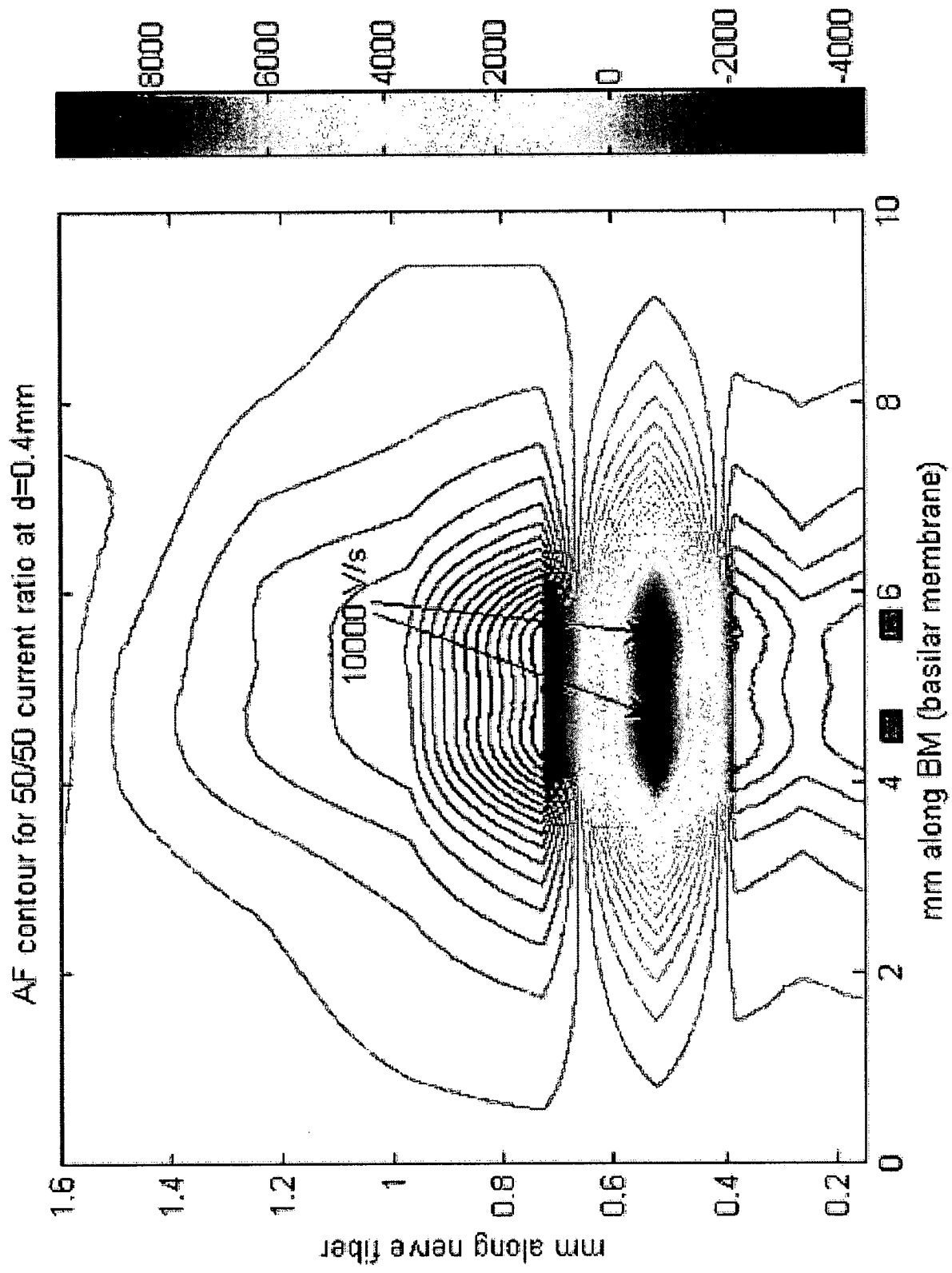


Figure 9
Click here to download high resolution image

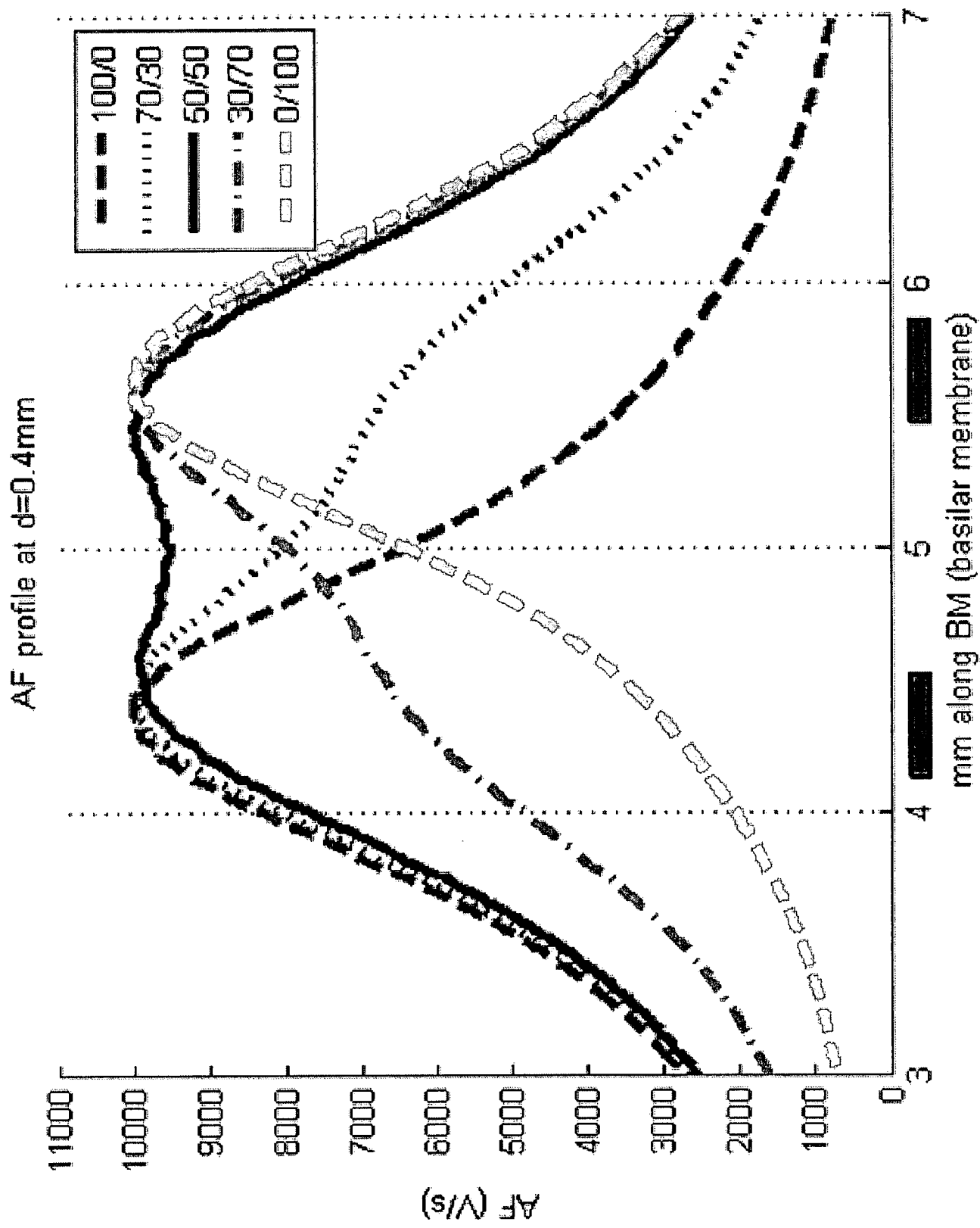


Figure 10
Click here to download high resolution image

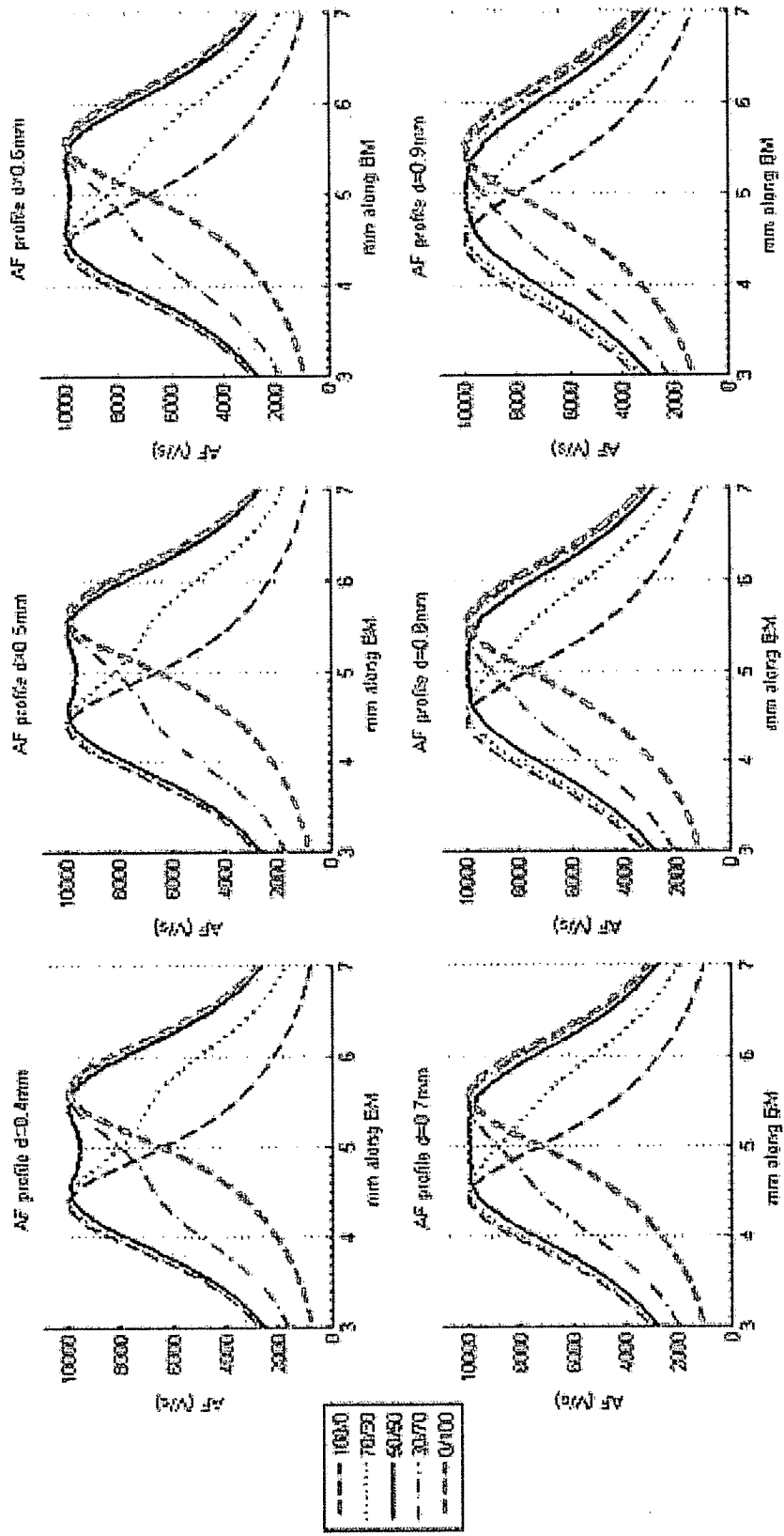


Figure 11abc
Click here to download high resolution image

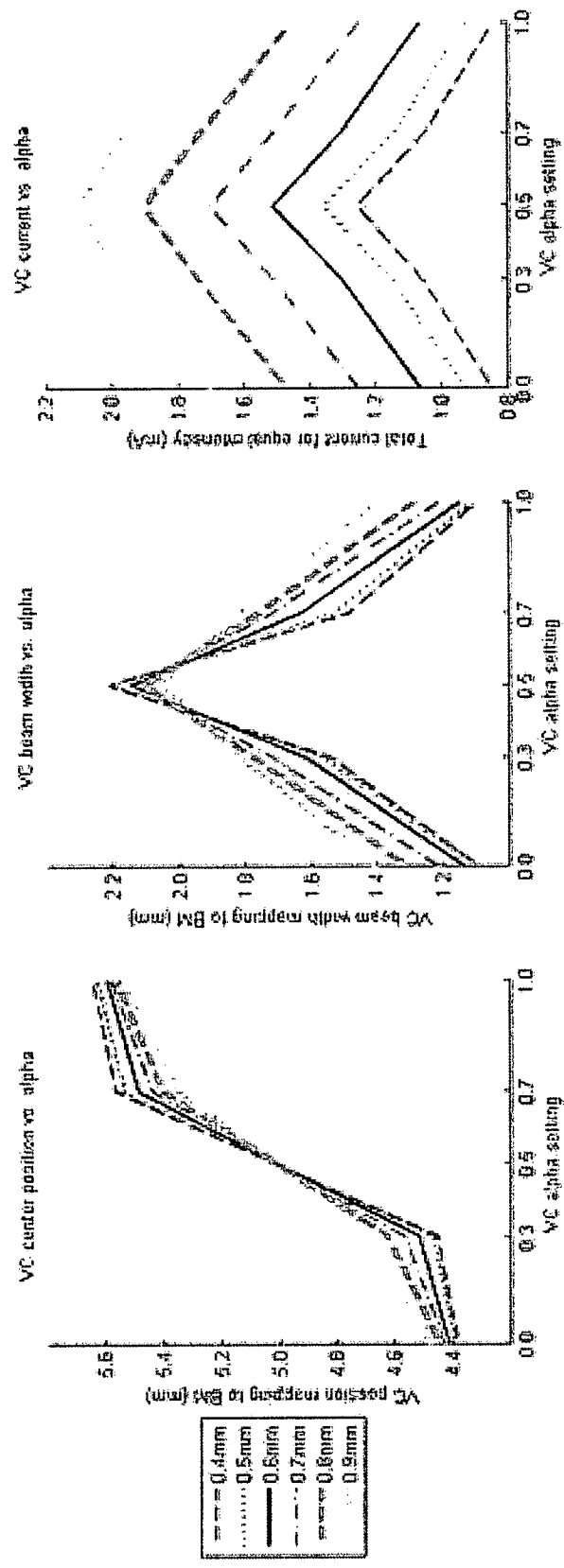


Figure 12
Click here to download high resolution image

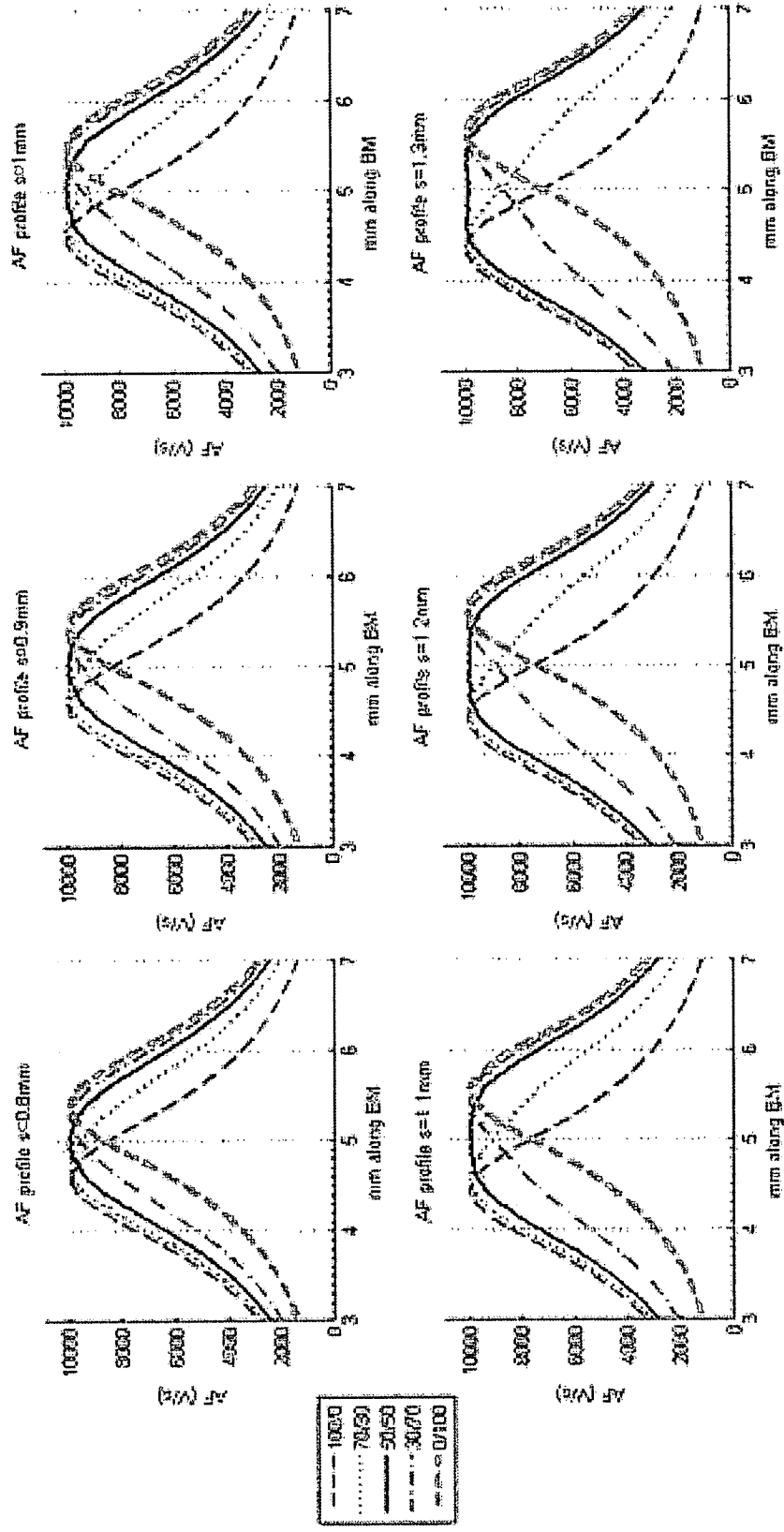


Figure 13abc
Click here to download high resolution image

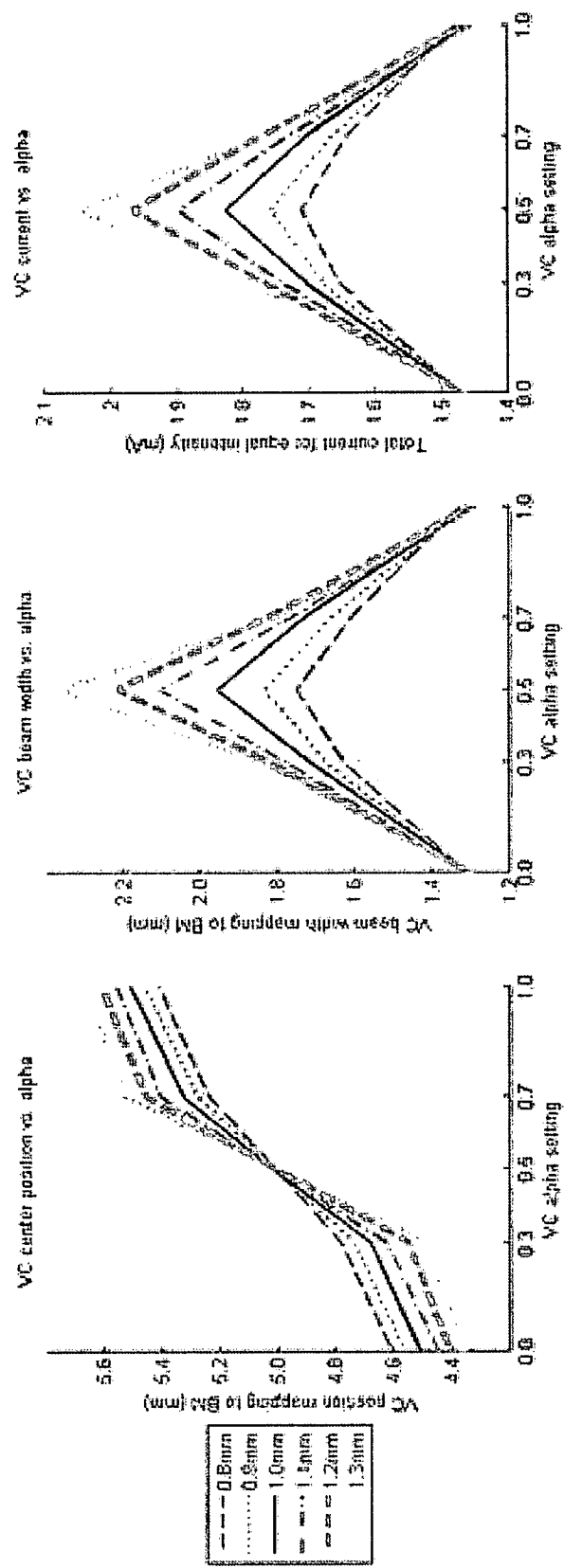


Figure 14abc
Click here to download high resolution image

